



**Environmental
Science**
Processes & Impacts

**Photochemistry of Oil in Marine Systems: Developments
Since the Deepwater Horizon Spill**

Journal:	<i>Environmental Science: Processes & Impacts</i>
Manuscript ID	EM-CRV-06-2023-000248.R1
Article Type:	Critical Review

SCHOLARONE™
Manuscripts

1
2
3 Environmental significance statement
4

5 Photochemistry of Oil in Marine Systems: Developments Since the Deepwater Horizon Spill
6

7
8 Critical Review
9

10 Oil is frequently released into the environment. Understanding of the fate and impact of oil
11 spills is still limited, and technologies to mitigate their impacts are insufficient. After the
12 Deepwater Horizon oil spill in 2010, research improved our understanding of the fate and
13 transport of oil spilled in marine systems. A limited group of studies focused on the impact of
14 sunlight on spilled oil, completely changing our understanding of the importance of sunlight in
15 oil spills. Assessment and remediation strategies must be updated to account for sunlight
16 impacts. This review covers the oil photochemistry work completed after the Deepwater
17 Horizon spill and provides oil spill and environmental professionals resources for finding and
18 applying current knowledge to oil spill challenges.
19
20
21
22
23
24
25
26
27
28
29
30
31
32
33
34
35
36
37
38
39
40
41
42
43
44
45
46
47
48
49
50
51
52
53
54
55
56
57
58
59
60



Double-Anonymised Title Page

Authors:

Mohamed Elsheref, Lena Messina, Matthew A. Tarr

Affiliations:

Department of Chemistry, University of New Orleans, New Orleans, LA 70148

Photochemistry of Oil in Marine Systems: Developments Since the Deepwater Horizon Spill (DWH)

Abstract

Oil spills represent a major source of negative environmental impacts in marine systems. Despite many decades of research on oil spill behavior, photochemistry was neglected as a major factor in the fate of oil spilled in marine systems. Subsequent to the Deepwater Horizon oil spill, numerous studies using varied approaches have demonstrated the importance of photochemistry, including short-term impacts (hours to days) that were previously unrecognized. These studies have demonstrated the importance of photochemistry in the overall oil transformation after a spill and more specifically the impacts on emulsification, oxygenation, and microbial interactions. In addition to new perspectives, advances in analytical approaches have allowed an improved understanding of oil photochemistry after maritime spill. Although the literature on the Deepwater Horizon spill is extensive, this review focuses only on studies relevant to the advances in oil photochemistry understanding since the Deepwater Horizon spill.

Introduction

The marine system is an extremely vital component of our environment. It is critical for human survival, serving as an important source of crucial human needs such as food and energy resources; thus, keeping it free of contamination is a chief priority.¹ Due to the tremendous amount of petroleum extracted and transported, there is a significant risk of spillage into maritime systems. Natural seeps^{2,3}, tankers⁴, offshore platforms^{5,6}, and pipelines⁷⁻⁹ can all be sources of oil release into the environment. The average annual estimated amount of oil entering marine systems is approximately two million tons.¹⁰

The United States Department of Energy estimates that over one million gallons of petroleum are released into US waters each year from oil production facilities.¹¹ The Deepwater Horizon (DWH) spill on April 20, 2010 was one of the most disastrous oil spills in US history. Several million barrels were spilled at the sea floor during about three months of continuous release at 1.5 km depth.¹²⁻¹⁶ This huge amount of spilled oil preceded numerous research investigations, leading to broadening of our understanding of the different weathering processes, including photochemistry. Enrichment of the oxygenated content of weathering oil occurs through different pathways, including evaporation (increase of concentration of the originally present oxygenated hydrocarbons), biological oxygenation, and photochemical oxygenation.¹⁷

Crude oil is a complex mixture of thousands of hydrocarbons and trace amounts of heteroatoms such as sulfur, nitrogen, oxygen, and metals.¹⁸ The molecular masses of crude oil organic molecules and their refined derivatives range from 16 Da for methane to more than 1000 Da for asphaltenes.¹⁹

An oil spill can result in a wide range of consequences across different areas, including environmental, human health, and economic sectors. Direct skin contact with oil components containing carcinogenic substances can cause serious health problems such as neurological difficulties.²⁰ Furthermore, when volatile substances are released into air during a spill and subsequently inhaled, they can impair health and exacerbate pre-existing ailments.²¹ Moreover, ingestions of oil contaminated seafood or drinking water can also cause health concerns.²² On a

1
2
3 commercial level, reduced production, mortality of commercial species, and harvesting closures
4 result in direct losses for fisheries and aquaculture.²⁰ As a result, businesses that rely heavily on
5 the fishing industry, such as distributors and supply companies, may be adversely affected.
6 Research on the toxicity of spilled oil following the DWH revealed valuable insights, although
7 additional study is needed to gain sufficient understanding. Links between oil presence and
8 negative effects on biological diversity and macrofauna were established using a sediment
9 quality triad.²³ Moreover, evaluating aquatic contamination after a spill relies on established
10 protocols and toxicity experiments, yet challenges exist in their proper execution.²⁴
11
12

13 From the moment an oil spill occurs in a marine environment, the oil undergoes physical
14 fractionation of its components into oil, water, and air phases, causing changes in composition,
15 fate, and impacts.^{25,26} Weathering processes include physical processes as well as chemical and
16 biological processes that change the oil profile.²⁷⁻²⁹ Dissolution and evaporation commence
17 immediately, while photooxidation begins as soon as the oil is exposed to solar irradiation,
18 increasing its compositional complexity.³⁰⁻³⁴ Increased water solubility and elevation of boiling
19 points both result from production of more oxygen functionalized compounds through biological,
20 thermal, or photochemical reactions. The onset of emulsification is considered a secondary
21 process that begins several hours after the spill occurs and may continue for a year or longer.
22 Biodegradation is often regarded as being on par with emulsification in terms of relevance,
23 beginning several hours after a spill for highly bioavailable compounds and extending for years
24 for more recalcitrant species.³⁵⁻³⁷ Physical changes caused by evaporation and dissolution shift
25 the distribution of petroleum hydrocarbons and affect the physical properties through
26 evaporation of low molecular weight species, such as shorter alkanes, leaving the higher
27 molecular weight hydrocarbons in the oil phase.¹⁵ Based on the report of Freeman and Ward,³⁸
28 photodissolution accounted for the fate of 3-17% of DWH surface oil. Fate estimates for other
29 processes were 1-12% for marine oil snow formation, 0-12% for biodegradation, 10-30% for
30 stranding, 10-46% for evaporation, 33-75% for entrainment, and 3-18% for recovery and
31 burning.
32
33
34

35 Photooxidation is an environmental process in which sunlight drives chemical reactions that
36 generally involve oxygenation of oil to produce more water soluble and more polar compounds.
37 Previously, photooxidation was believed to be a minor and ineffective secondary weathering
38 process that required weeks to months to occur.³⁹ According to these prior beliefs, the relative
39 importance of photooxidation was predicted to be less than evaporation, emulsification, and
40 biodegradation. Prior to the Deepwater Horizon (DWH) oil spill, it was widely assumed that
41 photooxidation had a minimal effect on the outcome, transport, or response of oil spilled into
42 water, as it only affected a small part of the released oil.⁴⁰ Among the studies of oil weathering
43 processes prior to DWH oil spill, relatively few articles concentrated on the photooxidation
44 process. Most of these studies were performed under controlled laboratory conditions.^{41,42}
45 Additionally, there were few comparisons between laboratory experiments and samples collected
46 from actual spills, and no prior research established a connection between the amount of
47 oxidized material produced and the time during which oil remained on the ocean surface.⁴⁰ In
48 addition, oil photochemistry research was primarily focused on PAHs, which account for only a
49 portion of crude oil molecules. Consequently, there was insufficient focus on other
50 photooxidation reactions, including those involving photosensitized reaction of oil compounds
51 that do not absorb solar radiation directly. The analytical technology prior to the DWH spill
52 could not effectively identify the photoproducts or compound classes at the
53
54
55
56
57
58
59
60

1
2
3 molecular level, largely because photoproducts are outside the operating window of
4 gas chromatography (GC).
5

6 This review covers the oil photochemistry studies since the DWH spill and includes discussion
7 of the photochemical processes, the effects of catalysts, the observed photoproducts, the impacts
8 on biological systems, and analytical techniques that were critical to improving our
9 understanding of how sunlight impacts oil spilled in aquatic systems. Because so many advances
10 have occurred in understanding oil spill photochemistry, it is important for the broader oil spill
11 research community to become familiar with its true impacts on spill fate and consequences.
12 The articles discussed in this review provide a gateway to such understanding.
13
14

15 **Oil Photochemistry**

16 *Photooxidation process and laboratory simulation techniques*

17
18 Comprehensive investigations into weathering processes affecting spilled oil in marine systems,
19 including photochemical reactions, have been carried out to explore a range of facets including
20 molecular transformations, transport, fate, and the potential toxicity of the newly generated
21 molecules. In laboratory-based studies, simulated sunlight is used in order to mimic natural
22 sunlight. When choosing the artificial radiation source, several factors should be considered such
23 as similarity to the solar spectrum, exposure period, and intensity, all of which should be
24 compatible with natural field conditions of the geographic area under study. Some studies have
25 focused on gathering samples of naturally weathered oil and monitoring the changes in oil profile
26 as well as the production of new polar compounds.⁴³⁻⁴⁵ Other studies used laboratory methods
27 with artificially weathered oil such as ultraviolet (UV) and visible light lamps.⁴⁶⁻⁵²
28
29
30

31 Freeman and Ward recently studied solar impact on spilled oil dissolution as a function of
32 photon dose and wavelength.³⁸ This study found that photodissolution rates were most dependent
33 on oil film thickness, season, latitude, and wavelength. An estimated 8% of DWH surface oil was
34 subject to photodissolution. This publication discusses key parameters needed to extrapolate from
35 laboratory to field conditions. While actinometry is an effective tool for measuring actinic dose,
36 it is often replaced by the use of light meters along with the spectral properties of the radiation
37 source.
38
39

40 Following the DWH oil spill in 2010, Tarr et al. conducted several investigations on the spilled
41 oil in the Gulf of Mexico.^{47-51,53,54} In a study aimed at observing the formation of aldehydes and
42 ketones through photo-exposure in an aquatic environment, Cao and Tarr⁵⁵ studied three
43 different types of oil: Macondo crude oil (MC252), a surrogate oil (A0067T) from BP, and a
44 SRM 2717a oil. They subjected the oils to simulated sunlight over seawater using an Atlas CPS+
45 simulator for a maximum of 24 hours, with a solar intensity that was 1.3 times AM 1.5 at a
46 temperature of 27°C. Air mass 1.5 (AM 1.5) is a widely accepted standard for the solar intensity
47 and wavelength dependency of natural sunlight at the Earth's surface in North America,
48 corresponding to a total irradiance of 1000 W/m². The authors observed a rise in the oxygen
49 content of the oil photoproducts in the water phase under oil after collecting and derivatizing
50 with 2,4-dinitrophenylhydrazine (DNPH). This increase was in the form of oxygenated
51 functionalized compounds such as dicarbonyl, hydroxy carbonyl, and oxo-carboxylic acids.
52
53
54
55
56
57
58
59
60

1
2
3 Niles *et al.*⁵⁶ investigated the molecular characterization of oil-soluble species (ketone/aldehyde)
4 in a photooxidation microcosm simulation study. Comparing the transformations produced in the
5 lab to those from field samples, there were structural similarities between ketones and aldehydes.
6 This work utilized an ATLAS Suntest CPS solar simulator with artificial sunlight for 48h at 27
7 °C. A thin film of SRM 2779 crude oil was created by spreading 385 µL of oil on top of 50 mL
8 of sterilized 70% artificial seawater, resulting in a film with a thickness of 120 µm. This study
9 included a microcosm investigation of biodegradation for the purpose of detecting the primary
10 source of the production of aldehydes and ketones. The authors concluded that photooxidation is
11 the primary process for the generation of oxygenated hydrocarbon species in weathered oil,
12 whereas the oil samples which underwent biodegradation did not produce such products.
13
14

15
16 Zito and Tarr⁵¹ examined the creation of hydroxyl radical from crude oil obtained from the
17 Deepwater Horizon spill under simulated solar radiation with an Atlas CPS+ solar simulator. The
18 research also evaluated the impact of photocatalysts and the contribution of oxygen in the
19 creation of hydroxyl radicals. For each sample, 100 mg oil were spread on top of 10 mL of water
20 to give a 60 µm oil thickness. The oil samples were subjected to radiation over a duration of 3 to
21 24 hours at 765 W/cm² within the 300-800 nm range, equivalent to 1.26 times the full sunlight
22 intensity of 1000 W/m² for the full spectrum AM 1.5. The results indicated that when exposed to
23 sunlight, the oil produced a significant quantity of hydroxyl radicals. Additionally, the utilization
24 of TiO₂ photocatalyst nanoparticles had a significant impact on the rate of hydroxyl radical
25 formation, leading to an increase in many instances.
26
27

28
29 Zito and Tarr⁴⁹ also utilized the Atlas CPS+ solar simulator to gain insight into the fundamental
30 mechanisms involved during the interaction between sunlight and oil after a spill. In this study,
31 the photochemical creation of singlet oxygen was observed from oil both over seawater and pure
32 water. The oil samples used were either collected from the surface of the Gulf of Mexico or
33 obtained from the National Institute of Standards and Technology (NIST). All samples were
34 spread as a thin film (~60 µm) of oil on the surface of 10 mL of either seawater or pure water
35 that contained furfuryl alcohol as a probe for singlet oxygen production. The samples were then
36 exposed to simulated solar radiation for a duration ranging from 15 minutes to 1 hour. The
37 amount of singlet oxygen produced was quantified by monitoring the decrease in furfuryl alcohol
38 and the formation of 6-hydroxy(2H)pyran-3(6H)-one. The results showed that when exposed to
39 sunlight, oil generates singlet oxygen. The addition of two different concentrations of TiO₂ to the
40 system did not alter singlet oxygen production. Furthermore, the generation of singlet oxygen in
41 oil films on water significantly impacted its fate.
42
43

44
45 A study done by Zito *et al.*⁵⁰ investigated the changes in water-soluble organic (WSO)
46 compounds from Macondo oil after exposure to simulated sunlight. The oil samples were spread
47 on top of pure water (10 mL over 100 mL pure water) in a jacketed beaker covered with a quartz
48 lid. The samples were allowed to equilibrate in the dark for 7 days before being exposed to
49 simulated solar radiation from an Atlas CPS+ at 27°C, with stirring, for a duration of 12 hours.
50 The same method was used to create a non-irradiated control in the dark. Another sample of oil
51 was removed and re-equilibrated in the same way, then the WSO fraction was exposed to
52 radiation after 12 hours. The authors found a higher level of oxygen-containing compounds in
53 the irradiated samples compared to the dark control. The presence of higher-order oxygen classes
54
55
56
57
58
59
60

(molecules with multiple oxygen atoms) suggests that the continued and sequential addition of oxygen to petroleum molecules takes place over the irradiation course.

The AtlasSuntest CPS+ outfitted with a 1500 W air-cooled xenon arc lamp was used by King et al.⁵⁷ for studying the photochemical transformations that occurred in DWH crude oil. A mixture of toluene and pentane (1:20) with sonication was used to disperse thicker oil samples on the water surface, forming a homogenous thin oil film before irradiation. Minor losses of alkanes were reported, in keeping with earlier investigations, while significant degradation of polycyclic aromatic hydrocarbons (PAHs) occurred. Moreover, the toxicity of the collected aqueous phase increased considerably as the photoirradiation processed. King et al.⁵⁸ utilized the same method by using simulated sunlight for irradiation of oil in the presence and absence of TiO₂ for assessing the enhancement in oil photodegradation. During 12 h of irradiation, about 60% loss of the fluorescence was observed at the excitation and emission maxima along with 80-90% loss of the higher molecular weight PAHs within the same period. The addition of the catalyst had a substantial effect on the solubility and toxicity of the aqueous layer after irradiation.

Zito et al.⁵⁹ studied the generation of oxygenated petroleum species and their migration from the oil to the interfacial layer and further to water under simulated sunlight. The study monitored changes in composition in each fraction from thin films (120 μm) of Macondo oil spread over 50 mL of seawater that had been exposed to simulated sunlight beforehand, using an Atlas Suntest CPS+ solar simulator for 24 hours (which was equivalent to 6 days of natural sunlight). The authors detected increasing polarity due to increased oxygen content. However, the overall polarity was also dependent on the carbon number, with larger molecules with the same oxygen content being less polar. Ward et al.⁶⁰ tracked the formation of oxygen-containing functional groups using δ¹⁸O as a tracer of hydrocarbon partial photooxidation. In this study, the authors exposed SRM 2779 oil samples from the DWH oil spill to irradiation in an Atlas XLS+ solar simulator with a long-arc Xe lamp for 24 hours, with and without dissolved oxygen present, and analyzed the stable oxygen isotope composition (δ¹⁸O) in the resulting products. The authors concluded that the main source of oxygen added through photochemical processes is atmospheric oxygen, not from seawater. Additionally, they found that the kinetic isotopic fractionation of dissolved oxygen that is photochemically incorporated into hydrocarbons is not influenced by the physical and chemical properties of organic carbon (such as crude oil or dissolved organic carbon), suggesting that different types of organic carbon follow a similar pathway during photochemical oxidation.

Arekhi et al.,⁶¹ examined the efficiency of economical LED light sources (a full-spectrum LED light and a UV-A LED light) for conducting a laboratory-scale, PAHs photodegradation experiment and compared the results with natural sunlight. According to the authors, the photodegradation primarily contributed to the loss of high molecular weight (HMW) PAHs, whereas lighter PAHs underwent degradation through both photodegradation and evaporation mechanisms. Moreover, the photodegradation rates of PAHs induced by full-spectrum LED light closely matched those induced by natural sunlight. In contrast, the UV-A LED notably expedited the photodegradation rates of PAHs, especially high molecular weight PAHs. Additionally, the UV-A LED light resulted in photodegradation rate constants for HMW PAHs that were approximately two to three orders of magnitude greater than those observed under sunlight and full-spectrum LED light. Hence, the UV-A LED light proved to be a cost-effective light source for investigating PAHs photodegradation processes in a laboratory setting. Here the study offers

1
2
3 valuable insights into the comparative effectiveness of two different light sources for carrying
4 out experiments on PAHs photodegradation. However, restricting the study to only two LED
5 light sources in comparison to natural sunlight does not provide a meaningful basis for
6 comparing other artificial light sources or variations in light intensity, highlighting the necessity
7 for additional research to examine the effectiveness of alternative affordable LED types.
8 Moreover, the experiments were conducted under a controlled laboratory environment, which
9 may not completely replicate the intricate environmental conditions. Conducting field
10 investigations to validate the findings of this laboratory-based study and evaluate the suitability
11 of inexpensive LED light sources for PAHs photodegradation would be of great significance.
12 The primary emphasis of the study was on the photodegradation of HMW PAHs without
13 extensive investigation of the degradation of lighter PAHs or other contaminants that might be
14 present in actual spill scenarios.
15

16
17 Simulated solar irradiation in a lab setting was also used for assessing the role of the
18 photooxidation process in fingerprinting of spilled oil in the ecosystem. For instance, Radović et
19 al.⁶² utilized natural sunlight and an artificial Xe lamp on a laboratory scale to examine the
20 photooxidation of two different types of oils for fingerprinting purposes. The authors gathered
21 samples of weathered Prestige oil that were seen in the ocean or washed up on shore during the
22 years 2003 and 2004. Another oil sample was obtained from the Macondo oil spill collected
23 twice from oil residue on rock fragments, in April 2011 and August 2012. The samples were
24 subjected to a Suntest CPS flatbed Xe-exposure system, which was equipped with a 1500B NrB4
25 Xe lamp that was operated at 507.5 W/m². The data obtained from the laboratory and field tests
26 of the Deepwater Horizon oil and the heavy fuel oil from the Prestige tanker spill were used to
27 enhance the understanding of the standard fingerprinting methodology.
28
29
30

31 Saeed et al.,⁶³ used the Suntest XLS Sunlight Exposure System, equipped with a xenon lamp, to
32 investigate how various environmental factors impact the photodegradation of PAHs in the
33 water-soluble fraction (WSF) of Kuwait crude oil in seawater. The study examined the influence
34 of various factors such as temperature, light intensity, dissolved oxygen levels, and the
35 presence/absence of environmental sensitizers such as anthraquinone. The authors pointed out
36 the substantial effect of all the studied parameters on the degradation rate of PAHs. Most of the
37 PAHs demonstrated a high rate of degradation at a temperature of 15°C and an oxygen level of 4
38 ppm. However, there was a difference in the degradation rate between PAHs with lower
39 molecular weight and those with higher molecular weight. The degradation of PAHs with lower
40 molecular weight was found to occur rapidly under intense light (500 W/m²) and in the presence
41 of environmental sensitizers at a temperature of 30°C. On the other hand, PAHs with higher
42 molecular weight degraded quickly under even more intense light (750 W/m²) and in the
43 presence of sensitizers at a higher temperature of 40°C. The results of the linear regression
44 analysis obtained in this study indicated that, for most of the oil compounds, light intensity had
45 the largest effect on their degradation rates. Liu et al.⁶⁴ conducted an experiment to examine the
46 dissolution and photodegradation of two types of crude oil in seawater by exposing a solution
47 containing the water-soluble fraction to radiation from a 300 W Mercury lamp in a cylindrical
48 reactor. The lamp was enclosed by a quartz jacket and a water-cooling system was used to
49 regulate the temperature at 20 ± 1°C. During the experiments, the irradiation intensity was kept
50 constant at 40 mW/cm². To simulate sunlight, a special glass that cut off wavelengths below 290
51 nm was placed between the lamp and the solution. The results of the study revealed that the
52 presence of dissolved organic matter (DOM) in seawater increased the dissolution of crude oil.
53
54
55
56
57

1
2
3 Furthermore, the photodegradation of the water-soluble fraction was found to follow a pseudo-
4 first order kinetic pattern.
5

6
7 A study conducted by Fathalla and Andersson⁶⁵ investigated the photodegradation of polycyclic
8 aromatic sulfur compounds (PASHs) in an Egyptian crude oil. The study involved dissolving 32
9 mg of isolated PASHs in 2 mL of cyclohexane, then adding the mixture to 50 mL of distilled
10 water that had been saturated with oxygen. The system was operated in a closed vessel to
11 minimize evaporation. The solar simulation was performed using Duran glass, which removed
12 wavelengths below 300 nm in order to imitate natural sunlight more closely. The flask was
13 exposed to radiation using a medium-pressure mercury lamp. A control sample consisting of
14 cyclohexane and water with 1.5 mg of anthraquinone was prepared and treated in the same
15 manner as the irradiated PASH fraction. The photoproducts detected in the sample included a
16 diverse array of sulfonic acids, aliphatic and aromatic acids, and alcohols.
17
18

19
20 Griffiths et al.⁴⁶ conducted a study to examine the molecular level compositional changes in a
21 light-sour crude oil sample after exposure to simulated sunlight using two different sources of
22 radiation. The study utilized a UV emission source with a wavelength of 254 nm, and a SoLux
23 bulb with a color temperature of 4700 K and 35 W output. The SoLux bulb was selected because
24 its light profile closely resembles that of solar irradiation. Meanwhile, the UV source was chosen
25 to investigate the effects of UV exposure, which falls outside the profile of the SoLux bulb and
26 outside the solar spectrum at the Earth surface. For irradiation, 10 mL of crude oil was put on a
27 150 mm watch glass at 11 cm away from a SoLux or UV light source for 39 days. The authors
28 found that the profile of PAHs did not change significantly in comparison to the heteroatom-
29 containing compounds, which were more prone to photooxidation. Additionally, among the
30 heteroatom-containing compounds in the mixture, the sulfur-containing compounds with a low
31 number of double bond equivalents were found to be the most reactive. The authors concurred
32 with many other studies on oil photochemistry, noting that after undergoing photooxidation, the
33 petroleum compounds were likely to become more soluble and toxic.
34
35

36
37 Kim, et al.⁶⁶ investigated the compositional variations in the Hebei Spirit oil spill (HSOS) during
38 the disaster. The oil sample (0.1 g) was spread on top of filtered seawater (10 mL) in a 20 mL
39 precleaned vial and exposed to UV radiation for time intervals of 6, 12, 24, 48, and 72 hours. A
40 reference sample was created using the same method; however, it was wrapped with aluminum
41 foil to prevent exposure to UV. The UV-A, UV-B, and UV-C irradiance from the lamp was
42 measured at 19.9, 1.91, and 0.21 W/m², respectively and the irradiation system temperature was
43 kept at a range of 15–20 °C. The proportion of compounds with a double bond equivalence value
44 (DBE) ≥ 5 increased, while the quantity of compounds with a DBE < 5 decreased. In the lab
45 studies, the total ratio of the abundance of compounds with DBE < 5 and DBE ≥ 5 showed a
46 negative exponential relationship with the duration of UV exposure. Spilled oils collected from
47 the environment showed the same pattern. As a result, this ratio can be used to evaluate spilled
48 oils weathering degree. However, the UV radiation used in this study includes regions outside of
49 the solar spectrum. Zhang et al.⁶⁷ utilized UV radiation to investigate the photodegradation of
50 oily wastewater in the presence of nano-TiO₂ with the use of a 500 W mercury lamp. To keep the
51 lamp cool, it was housed inside a quartz tube and surrounded by a circulating water jacket. The
52 lamp and the tube were placed in the photoreactor cell. A magnetic stirrer was used to keep the
53 sample (1 g jet fuel and 0.1 g TiO₂) mixed. Following UV exposure, the sample was extracted
54
55
56
57
58
59
60

1
2
3 with n-hexane to measure the remaining oil concentrations in the water. The authors concluded
4 that after 1 h of irradiation, the photodegradation had reached 86%. Again, the use of UV
5 radiation may result in findings not appropriate for natural sunlit systems.
6

7
8 The simulated irradiation techniques reviewed in this section highlight the contribution of
9 photooxidation in generating a substantial quantity of water-soluble organics and reactive
10 oxygen species in oil-seawater systems. Additionally, the results emphasize the pivotal role of
11 photooxidation in degradation of larger PAHs, which are typically resistant to biodegradation.
12 This information enhances our understanding of how sunlight impacts the environmental fate and
13 impact of spilled oil, while also aiding in the development of effective oil spill responses.
14 However, simulated sunlight may not accurately replicate the conditions of natural sunlight,
15 especially if small differences in short wavelength radiation exist. Neglecting the effects of the
16 dynamic conditions of the natural environment where oil spills occur is another major weakness
17 of laboratory studies. Different temperatures, varying concentrations and distributions of oil,
18 day-night cycling, diffusion into large volumes of ocean water, and wave action are key factors
19 that have not been well addressed. In addition, a mass balance methods have not been widely
20 used to provide insights into the sources and pathways of hydrocarbon photo-oxidation. The
21 findings also have broader implications in tracking the cycling of a wide range of organic carbon
22 sources beyond oil spills.
23
24
25
26

27 *Impacts of environmental factors on photodegradation process*

28 The environmental factors in the spill area, as well as the oil composition, have substantial
29 effects on the fate and photodegradation of spilled oil. Once oil is introduced into marine
30 environment, it undergoes photochemical changes due to exposure to sunlight. Sunlight affects
31 the indigenous microorganisms through photooxidation processes that modify biological activity
32 in the spill area by enhancing some oil-degrading bacterial communities, which are capable of
33 utilizing the oil photoproducts.⁶⁸ Photooxidation also boosts the biodegradation process by
34 increasing the bioavailability of oil compounds in water.¹⁵
35
36

37 Photodegradation as well as other abiotic and biotic weathering processes are affected by the
38 temperature of the spill environment. According to Shankar et al.,⁶⁹ the impact of temperature on
39 photochemical reactions altered the rate of singlet oxygen and free radical formation. These
40 transient reactive species participate in the oxidation of other substances, such as natural organic
41 matter and dissolved inorganic matter, as well as the degradation of oil molecules.⁵¹
42 Furthermore, temperature was reported as a highly influential parameter in determining the
43 bioavailability of various oil fractions such as PAHs and alkanes. Freeman et al.⁷⁰ recently
44 reported on changes in temperature-dependent oil properties caused by photochemical
45 weathering. Sunlight exposure resulted in increased oil viscosity and water-soluble content and
46 decreased oil-seawater interfacial tension. Furthermore, these changes showed temperature
47 dependence, with weathered oil at 5°C having 16x higher viscosity than at 30°C and 7x lower
48 water solubility at the lower temperature.
49
50

51 The study conducted by Saeed, et al⁶³ investigated the influence of certain environmental factors,
52 including the existence or lack of sensitizers, temperature, light intensity, and dissolved oxygen
53 levels, on the photooxidation process and its impact on the degradation rate of PAHs in Kuwait
54 crude oil's water-soluble fraction in the Arabian Gulf region. The study detected a total of 43
55
56
57

1
2
3 different volatile organic compounds and 18 PAHs. The temperature had a significant impact on
4 the degradation of oil components. Furthermore, increasing light and dissolved oxygen enhanced
5 the degradation of PAHs. Moreover, in the deoxygenated WSF, the degradation rate at 30°C was
6 substantially higher than that at 15°C. Additionally, the degradation rate was enhanced in the
7 presence of a sensitizer. The authors highlighted that the latitude of the spill location had an
8 impact on the degradation of oil. Locations with hot weather and high light intensity at higher
9 latitudes will significantly contribute to oil photodegradation. Furthermore, biodegradation may
10 be hindered by the lack of nutrients in tropical and subtropical latitudes. Therefore, this study
11 established a foundation for forecasting the influence of location on the behavior of spilled oil.
12
13

14 The presence of marine snow in the oil spill area could have an impact on the oil fate. Marine
15 snow interacts with the spilled oil and dispersants, resulting in the formation and settling of
16 marine oil snow (MOS) and a buildup of flocculant. In a mesocosm simulation study that
17 investigated the degradation of oil in marine oil snow events following the Deepwater Horizon
18 oil disaster, Wozniak, et al⁷¹ found that as much as 47% of the signal from the MOS involved
19 degraded Macondo oil in the formation of MOS. Similar double bond equivalents but higher
20 oxygen contents were found in some of the detected formulae, accounting for the similarities of
21 MOS to the degraded oil components. The settling of the formed MOS to the ocean floor, the
22 high presence of hydrocarbon-degraders, and the low levels of light at the ocean floor indicate
23 that biodegradation is the primary factor responsible for oil degradation in the presence of marine
24 snow in the spill environment, rather than photooxidation.
25
26

27 Harsha et al.⁷² utilized complementary non-targeted and targeted techniques, including high-
28 resolution mass spectrometry, fluorescence excitation-emission matrix spectroscopy, and liquid
29 chromatography-triple quadrupole mass spectrometry, to monitor how the composition of
30 hydrocarbon oxidation byproducts (HOPs) from Cook Inlet, Alaska crude oil and diesel changed
31 over time due to variations in fuel types and exposure durations. The results showed that the
32 HOPs from crude oil exhibited a higher aromatic nature and those from diesel were more
33 aliphatic. The study also reported the presence of naphthenic acids in HOPs. Furthermore, HOPs
34 generated from Cook Inlet crude oil were observed to have relatively lower levels of oxidation,
35 being more saturated and aromatic, whereas those originating from diesel were predominantly
36 aliphatic. Fluorescence excitation-emission matrix spectroscopy revealed six unique chemical
37 features of HOPs, including two unique petroleum signatures. The molecular composition
38 classifications of HOPs demonstrated that in high-latitude environments, both crude oil and
39 diesel yield relatively less oxidized, saturated, and aromatic compounds under the influence of
40 sunlight. The findings of this study contribute to understanding the potential ecological
41 consequences of HOPs from crude oil and diesel providing a comprehensive approach for
42 monitoring their compositional changes in spill events and revealing their variations based on
43 fuel types and the duration of exposure to light. The study reports the molecular signatures of
44 naphthenic acids which have raised concerns due to their rapid transport and difficulty of
45 detection by conventional techniques. The paper addressed a broader range of HOPs and
46 correlating non-targeted and targeted methods, as a result, it deepens our comprehension of the
47 impacts of an oil spill in Cook Inlet. However, the study did not provide information about the
48 toxicity of HOPs to aquatic organisms, limiting our comprehension of their potential ecological
49 repercussions. Therefore, in forthcoming research, it is crucial to explore the toxicity of HOPs on
50 aquatic organisms as well as impacts of latitude on oil photochemistry.
51
52
53
54
55
56
57
58
59
60

1
2
3 Yin et al.⁷³ provided a dataset spanning four years documenting how PAHs trapped within the
4 residual oil buried along Alabama's beaches changed over time following the DWH oil spill. As
5 of August 2014, the research determined that the DWH oil was still retained along Alabama's
6 shorelines in submerged oil, primarily as surface residual oil balls (SRBs). The chemical analysis
7 revealed that a range of PAHs from the spilled oil had undergone weathering to varying degrees,
8 ranging from 45% to 100%, during the period when the oil was located in the open ocean system
9 of the Gulf of Mexico. Light PAHs, such as naphthalenes, were fully depleted, while heavy
10 PAHs, such as chrysenes, were only partially depleted by about 45%. The rate of PAHs
11 weathering significantly decreased once the oil was buried within the partially-closed SRB
12 environment. The data also suggested that when the oil was floating over the ocean, the
13 predominant mechanism responsible for PAHs removal was evaporation. However, it's possible
14 that photodegradation and other physico-chemical processes may have contributed to some
15 additional weathering. The study examined spatial differences in PAHs concentrations along the
16 coast of Alabama, revealing that all SRBs located on the beaches had undergone comparable
17 forms of weathering processes. Overall, the long-term monitoring data shared in this study offer
18 significant insights into the fate of PAHs following the DWH oil spill along Alabama's coast.
19 The results highlight the persistence of submerged oil, particularly in the form of SRBs, along
20 Alabama's beaches even four years after the spill. Moreover, the study emphasizes the need for
21 continued monitoring and assessment of PAH levels in the beach system to grasp the enduring
22 effects on the environment and the organisms inhabiting these regions. Such submerged or
23 buried residual oil or oil transformation products may or may not be subject to further
24 photochemical processes depending on the location and release of material into the aqueous
25 phase.
26
27
28
29

30 John et al.⁷⁴ investigated the impact of sunlight exposure on the weathering rates of PAHs in
31 submerged oil mats (SOMs) along the Alabama shoreline. The results showed that the
32 weathering levels of higher molecular weight PAHs in SOMs were slower compared to when the
33 oil was floating over the Gulf surface due to the absence of sunlight-induced photodegradation
34 reactions. Additionally, the presence of sand particles in SOMs could potentially interfere with
35 photodegradation reactions. Several PAHs showed signs of weathering in the SOM samples.
36 These findings have practical implications for the management and remediation of oil spills
37 containing SOMs. While the study did not provide a comprehensive analysis of the potential
38 ecological impacts of the slower weathering rates of PAHs in SOMs, the photoproducts likely
39 behave similarly to those observed in other studies. The effects on marine organisms, however,
40 are likely altered by binding to SOM material. Additional research is needed to assess the long-
41 term persistence and potential ecological impacts of PAHs in SOMs, including their effects on
42 marine organisms and the overall ecosystem dynamics.
43
44
45

46 Treatment of spilled oil with chemical dispersants is another factor that contributes to oil fate and
47 degradation. The dispersants aid in the decomposition of surface oil slicks into tiny droplets,
48 resulting in the dispersal of oil components throughout the body of water.^{75,76} Zhao et al.⁷⁷
49 studied the photodegradation of dispersed petroleum hydrocarbons in a seawater-sediment
50 environment under the influence of three different chemical dispersants, Corexit 9500A, Corexit
51 9527A, and SPC 1000. The use of chemical dispersants for treating oil spills resulted in the
52 spread of petroleum hydrocarbons in water column and sediment. Under solar irradiation, the
53 dispersed oil hydrocarbon fractions degraded dramatically. In addition to photodegradation, solar
54 irradiation increased the relative abundance of alkylated PAHs compared to the parent PAHs.
55
56
57

1
2
3 The oil components, as well as the dispersant, can produce photosensitizers, which accelerate *n*-
4 alkane photodegradation. Additionally, both *n*-alkanes and PAHs present in dispersed water
5 accommodated oil were susceptible to degradation by simulated sunlight. The authors indicated
6 that both photodegradation and photo-facilitated alkylation of PAHs occurred at the same time.
7 The alkylation process increased the photoreactivity of *n*-alkanes and PAHs and consequently
8 increased degradation under solar irradiation. The dispersant may also improve PAH
9 photodegradation by improving their capacity to facilitate charge separation and increased
10 radical generation.⁷⁸
11
12

13 Ward et al.⁷⁹ conducted a research to examine the effect of photochemical oxidation on the
14 efficacy of aerially applied dispersants during the remediation of the DWH oil spill. The oil
15 samples were positioned on pre-burned 150 millimeter Pyrex petri dishes that were kept at a
16 stable optical path length during incubation and then subjected to artificial sunlight in an Atlas
17 Suntest XLS+ solar simulator for a duration for up to 24 hours. For the samples used in this
18 study, exposing the oil to sunlight reduced dispersant effectiveness far more than the impact of
19 evaporation. The efficiency of dispersants was reduced by 29-34% after 24 hours of exposure to
20 simulated sunlight. Additionally, when 8-30% of the starting oil quantity evaporated, there was a
21 reduction in dispersant efficiency by 3-7%. The authors attributed the role of photooxidation in
22 reducing dispersant effectiveness to chemical changes in the weathered oil rather than physical
23 changes like viscosity or density, which were minor in comparison to the change in chemical oil
24 profile. The authors also highlighted the effect of photooxidation on the efficacy of dispersants,
25 which should be considered in future studies on the effectiveness of chemical dispersants in oil
26 spill incidents.
27
28
29

30 Podgorski et al.⁸⁰ found that dispersant enhanced photodissolution of Macondo crude oil with a
31 doubling in no-volatile DOC observed in laboratory studies. A combination of fluorescence and
32 mass spectrometric analysis revealed that the oil-phase residual material after irradiation was
33 predominantly aromatic in the absence of dispersant and aliphatic in the presence of dispersant.
34 The composition of the dissolved material, however, showed no difference between with and
35 without dispersant. As found across numerous studies, the impact of sunlight alters the behavior
36 of the spilled oil, and the solar impacts must be incorporated into oil spill models.
37
38

39 Several studies have revealed important connections between photochemistry and environmental
40 factors. Photochemistry has been shown to be impacted by temperature, latitude, and surfactant
41 presence. Similarly, exposure of oil to sunlight changes its physical and chemical properties,
42 including density, water-solubility, ability to be dispersed, and bioavailability. The studies
43 referenced in this section have provided clear evidence for the existence of these relationships,
44 but detailed understanding of the connections is not complete. Furthermore, accepted oil spill
45 responses, such as skimming and dispersion, are impacted by photochemical weathering in ways
46 that are not fully understood. Without a clear understanding of how sunlight impacts the efficacy
47 of other remediation methods, optimal spill response decisions cannot be made.
48
49

50 *The effect of catalyst on the photooxidation of crude oil*

51 Several laboratory studies have investigated the impact of photocatalysts on oil degradation.
52 Photocatalysts contribute to the production of reactive transient species, which enhance oil
53 degradation through both oxidation and increasing oil bioavailability. For example, using TiO₂
54 catalyst during oil photo-investigations can produce hydroxyl radicals, which oxygenate oil
55 molecules creating more polar compounds of higher water solubility and bioavailability.^{81,82}
56
57
58
59
60

1
2
3 Because photooxidation has not been sufficiently studied, the understanding of the role of
4 photocatalyst in promoting photooxidation is limited.
5

6 For studying the role of photocatalysts in degradation of oil-contaminated water, Zhang et al.⁶⁷
7 used a photocatalytic reactor system to conduct the photodegradation experiment. The authors
8 demonstrated that when the calcination temperature exceeded 400°C, some of the anatase TiO₂
9 particles transformed into the rutile phase, which has poor photocatalytic properties, leading to a
10 significant decrease in the photocatalytic activity of nano-TiO₂ (as shown in Fig 1). With mixed
11 anatase and rutile particles having sizes of about 10-100 nm, the photodegradation efficiency
12 achieved a maximum of 76% after 30 min and peaked at 86% at the experiment end. Extending
13 the experiment time had no discernible effects on the photooxidation enhancement.
14
15

16 Zito et al.⁵¹ studied the influence of photocatalyst on the formation of hydroxyl radicals by
17 employing benzoic acid as a chemical probe in the aqueous layer during a solar simulation
18 investigation of Deepwater Horizon oil samples. This study utilized both pure water and water
19 from the Gulf of Mexico to further examine the behavior of capturing hydroxyl radicals under
20 the probable influence of TiO₂. Table 1 displays the amount of hydroxyl radicals captured for
21 different water samples with varying levels of TiO₂ as a function of the irradiation time. When
22 comparing the amount of HO radicals captured in pure water at pH 3 with and without the
23 catalyst (9% TiO₂ nanotubes), a noticeable difference was observed. In pure water at pH 3, $(9.0 \pm$
24 $1.2) \times 10^{-7}$ mol of HO radicals were captured, while in the presence of 9% TiO₂ nanotubes at pH
25 3, only $(2.0 \pm 0.3) \times 10^{-7}$ mol of HO radicals were trapped. The total moles captured for a system
26 with 3% TiO₂ in pure water at pH 3 or 8 were comparable to those for a system without any
27 oxide. On the other hand, the trapping of radicals was significantly lower in Gulf of Mexico
28 water at pH 8 with 3% TiO₂. The utilization of TiO₂ catalyst nanotubes during irradiation
29 resulted in a higher reduction of PAHs in the oil phase, but a decrease in the concentration of
30 hydroxyl radicals in the aqueous layer under the oil film. However, with the presence of the
31 oxide, a corresponding increase in scavenging led to a decrease in the measured concentration of
32 hydroxyl radical in the aqueous layer. In another work for the same group, the impact of TiO₂
33 nanoparticles on singlet oxygen generation was examined by introducing the catalyst into the
34 system at two different concentrations.⁴⁹ The results showed that the addition of TiO₂ to the
35 spilled oil did not hinder the formation of singlet oxygen, but it did create new pathways for oil
36 degradation.
37
38
39
40

41 Brame et al.⁸³ conducted a study using food-grade titanium dioxide (FG-TiO₂) as an eco-friendly
42 friendly photocatalyst to examine the impact of the photocatalyst on enhancing the solubility and
43 biodegradability of Deepwater Horizon oil. The use of FG-TiO₂ led to a significant increase in
44 the amount of dissolved organic carbon (DOC) compared to UV exposure alone. The DOC rose
45 from 36 ± 1 mg/L to 81 ± 1 mg/L. This increase in soluble carbon content by 30-50 mg L⁻¹
46 during the 24-hour photocatalytic pre-treatment highlights the significance of addressing mass-
47 transfer barriers that hinder the bioavailability and biodegradability of weathered oil. Employing
48 FG-TiO₂ for 11 days under natural sunlight had no discernible effect on DOC concentrations
49 compared to the large effect attained with visible light and UV radiation treatment in lab studies.
50 The authors explained the cause of this difference by catalyst sinking in natural settings, as
51 opposed to remaining in the sample during stirring under laboratory conditions.
52
53
54
55
56
57
58
59
60

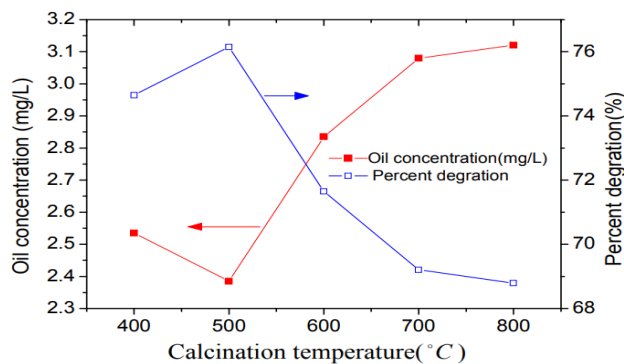


Fig.1. The photodegradation performance of TiO₂ calcinated at different temperatures, 30 min. Reprinted with permission from Zhang et al.⁶⁷

Oxide time(min)	Irradiation	Moles of HO [•] trapped ($\times 10^{-7}$)		
		NP water pH 3	NP water pH 8	Gulf water pH 8
3% TiO ₂	180	1.4 ± 0.2	0.5 ± 0.1	0.24 ± 0.04
	360	2.7 ± 0.4	1.1 ± 0.2	0.75 ± 0.03
	720	4.8 ± 1.2	2.3 ± 0.1	2.0 ± 0.2
	1440	8.9 ± 1.5	4.1 ± 0.6	2.5 ± 0.3
9% TiO ₂	180	2.0 ± 0.5	0.5 ± 0.1	0.41 ± 0.02
	360	3.3 ± 0.6	1.63 ± 0.03	1.1 ± 0.1
	720	7.3 ± 1.0	2.4 ± 0.5	2.4 ± 0.1
	1440	11.7 ± 3.0	7.0 ± 1.5	3.9 ± 0.6
3% TiO ₂	180	0.8 ± 0.1	0.33 ± 0.03	0.17 ± 0.04
	360	1.6 ± 0.3	1.5 ± 0.1	0.46 ± 0.02
	720	2.3 ± 0.2	1.5 ± 0.1	1.6 ± 0.1
	1440	2.5 ± 0.2	2.2 ± 0.1	1.8 ± 0.1
9% TiO ₂	180	1.1 ± 0.1	0.29 ± 0.04	0.1 ± 0.1
	360	1.6 ± 0.1	0.58 ± 0.03	0.53 ± 0.04
	720	2.9 ± 0.7	1.2 ± 0.1	1.3 ± 0.1
	1440	2.0 ± 0.3	1.4 ± 0.2	1.5 ± 0.4

Table 1. Moles hydroxyl radical produced by exposure of oil to simulated sunlight as measured by trapping with BA. Values presented are averages of three replicates ± one standard deviation. 120 IL of surface oil containing oxide was placed over 10 mL of water containing 10 mM BA and irradiated at 1.3 times solar noon intensity (AM 1.5) in a jacketed beaker maintained at 27 °C. Reprinted with permission from Zito et al.⁵¹

Saflou et al.⁸⁴ developed a floating magnetic nano Fe₃O₄-ZnO photocatalyst coated on lightweight minerals and used it under visible light to investigate the degradation of benzene in water as a model for oil components. The floating catalysts has advantages over the conventional catalysts due to the ability to remain with floating spilled oil and utilizing solar irradiation in proximity to the surface as well as proximity to atmospheric oxygen. Moreover, the ease for removal of the photocatalyst after remediation process is facilitated by floating. The prepared photocatalyst was supported on four different light minerals. The authors found that after a 180-minute exposure to simulated solar light at a pH of 7, the Fe₃O₄-ZnO on perlite (F.Z. Perlite) had the highest rate of benzene elimination at 85.4 ± 2.01% (as shown in **Fig 2**). The high efficiency of the F.Z. Perlite is attributed to the uniform dispersion of the small particles of F.Z.Pperlite

without agglomeration, which increased the number of available active sites on the material. The results of UV-Vis diffuse reflectance spectroscopy revealed that the band-gap energy in F.Z. Perlite was the lowest (3 eV) among the four catalysts used, which increased its ability to absorb visible light. Additionally, the heterojunction between ZnO and Fe₃O₄ effectively traps excited electrons and prevents recombination. Furthermore, the strong adsorption of benzene by F.Z. Perlite also increased the likelihood of its photodegradation.

Joodi et al.⁸⁵ studied the effect of C₃N₄ and ZnO as a floating photocatalyst supported on recycled polyethylene terephthalate (r-PET) for oil photodegradation. The results showed that increasing the amount of ZnO reduced the particle size, narrowed its distribution, and led to a more homogeneous morphology and greater surface area. As the amount of ZnO increased, the band-gap energy increased and the absorption of light in the visible and UV ranges improved. The extent of benzene removal rose from 78% in the presence of C₃N₄/r-PET to 99.74% in the presence of ZnO-C₃N₄/r-PET, resulting in the maximum degradation performance. Increasing the amount of photocatalyst generally results in an increase in active sites, but the excess amount of catalyst causes the floating catalyst particles to aggregate, which negatively affected the photocatalytic efficiency due to limitations in mass transport and photon absorption.

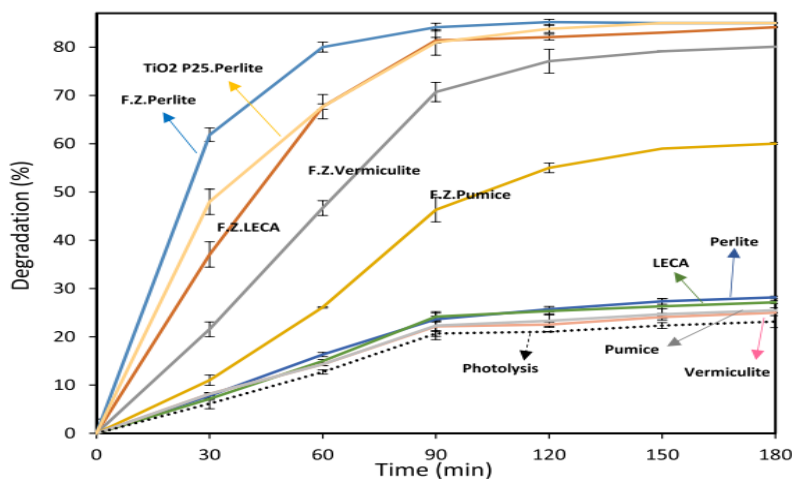


Fig.2. Photodegradation of benzene using Perlite, LECA, Pumice, Vermiculite, TiO₂ P25/Perlite, Fe₃O₄-ZnO/Perlite, Fe₃O₄-ZnO/LECA, Fe₃O₄-ZnO/Pumice, Fe₃O₄-ZnO/Vermiculite, the error bars represent the standard deviations of triplicate tests. The experiments were performed in benzene concentration of 5% v/v, catalyst loading of 0.4 g/L, and pH = 7. Reprinted with permission from Saflou et al.⁸⁴

Besides the effect of the catalyst amount, pH and initial benzene concentrations were also studied. The maximum extent of benzene degradation, 99.74%, was recorded at pH = 3. This observation indicated that the adsorption of benzene in the presence of ZnO-C₃N₄/r-PET is caused by van der Waals forces rather than electrostatic forces, due to the hydrophobic nature of r-PET. Additionally, as the initial concentration of benzene was increased from 1 to 5 vol. %, the removal noticeably rose from 49.76% to 99.74%. Increasing the initial concentration of the organic materials in general reduced the photodegradation rate due to turbidity in the aqueous system. The study also included investigation of the photocatalytic activity under some marine conditions such as wind, the type of light source, and salinity. The removal of benzene was found to be 93.13% in salt water, and 89.87% in marine water, which could be explained by the presence of impurities. Anions in seawater compete with the hydroxyl ions for adsorption to

1
2
3 active sites on the catalyst surface. Furthermore, in windy conditions, benzene evaporation was
4 more likely. The study also compared the effect of sunlight on benzene removal compared to the
5 simulated light source. The removal of benzene under natural sunlight was 97.36%, while it was
6 95.87% under simulated solar light. The authors attributed this slight difference to the nature of
7 sunlight, which combines visible and UV light, allowing the catalyst to absorb both, but this
8 degree of degradation was not achievable in the laboratory reaction test using a xenon lamp. The
9 authors also compared the removal efficiency of ZnO–C₃N₄/r-PET floating catalyst⁸⁵ with other
10 previously used catalysts in removal of petroleum components and organic pollutants.^{58,85–89}
11
12

13 Li et al.⁹⁰ studied degradation of a crude oil in seawater using two methods: N-doped
14 TiO₂/reduced graphene oxide (N/TiO₂/rGO) and traditional TiO₂, under UV light irradiation for
15 a period of 28 days. This study combined fluorescence spectroscopy, ultraviolet spectroscopy,
16 dissolved organic carbon (DOC) measurement, and GC-MS to monitor the photoproduct activity
17 within the water-soluble fraction (WSF). The results revealed that while nano-TiO₂ was highly
18 effective in breaking down aromatic compounds, it tended to form clusters, causing the crude oil
19 to also cluster and leading to the termination of the catalytic process after just 7 days.
20 Conversely, the N/TiO₂/rGO composite consistently dispersed the crude oil over the entire 28
21 days, resulting in a faster rate of photocatalytic degradation compared to TiO₂. When used
22 together, TiO₂ and N/TiO₂/rGO (4:1) demonstrated a cooperative catalytic effect on the
23 degradation process. The fluorescence intensities of WSF under the three different catalytic
24 systems recorded a peak on the 17th day and subsequently began to decline, indicating that
25 photodegradation of the fluorescent components was effective. Moreover, when comparing the
26 fluorescence spectra from the 7th to the 28th day, it was observed that the maximum peak
27 wavelength shifted towards longer wavelengths, which suggests that new fluorescent compounds
28 were formed through photochemical reactions.
29
30
31

32 While photocatalysts represent a potential pathway to enhancing degradation of spilled oil,
33 numerous barriers to their application remain. The impact of large quantities of these materials
34 in marine systems is a critical factor, and identifying materials that will effectively degrade oil
35 without residual environmental impact is challenging. In addition, TiO₂ and ZnO catalysts have
36 poor overlap with the solar spectrum, have greater density than water resulting in sinking, are
37 often inhibited by aggregation, and can be screened from sunlight by direct solar absorption by
38 the oil. While providing interesting information, these photocatalyst studies do not present
39 currently viable treatment strategies for aquatic oil spills.
40
41

42 *Photoproducts of weathered crude oil under solar irradiation*

43 Photooxidation is a weathering process responsible for substantial changes in the parent
44 compounds and the production of new compounds with different characteristics compared to the
45 original crude oil fractions. Many investigations focused on tracking these changes and looking
46 into the molecular transformations of the crude oil profile after a spill. Following the photo-
47 weathering of oil, the most significant alteration observed is the increase in the quantity of
48 oxygen-containing compounds. The study conducted by Hall et al.,⁹¹ involved analyzing data
49 obtained from GC-FID and TLC-FID measurements of various samples, including Macondo oil,
50 light weathered oil taken from the surface slick in May 2010, and a significantly weathered oil
51 collected from the Gulf of Mexico coastlines in Gulfshores, AL in November 2011. The authors
52 observed an increase in the proportion of the oxygenated hydrocarbons (referred to as OxHC),
53 which made up roughly 50% of the hydrocarbons analyzed, while at the same time, they noted a
54
55
56
57
58
59
60

1
2
3 decrease in the quantity of saturated and aromatic compounds. The authors employed GCxGC to
4 investigate the changes and identify any precursor compounds in 40 oil samples. They used
5 partial least squares regression to separate and identify the various chromatographic peaks, as
6 shown in **Fig 3**. The hypothesis that OxHC compounds are products of oil degradation is
7 supported by the high abundance of these compounds compared to 17a(H),21b(H)-hopane.
8 Approximately 80% saturated hydrocarbons such as tricyclic terpenoids, alkyl cyclopentanes,
9 alkylated bicyclic saturated compounds, alkyl cyclohexanes, and alkylbenzenes were identified
10 as the primary precursors, where the aromatic compounds were not believed to be the primary
11 precursors because they were present in lower concentrations in the crude oil.
12
13

14 A similar trend of increase in the oxygenated hydrocarbons has been observed by Zito et al⁵⁰ in
15 samples of DWH oil under simulated solar irradiation followed by FT-ICRMS analysis of water-
16 extractable material. The authors stated that oxygen was incorporated over a broad range of
17 carbon numbers and double bond equivalencies. In addition, exposure to sunlight caused both
18 acidic and basic species to undergo oxygenation. The samples subjected to sunlight contained
19 more higher-order oxygen classes (O₅–O₉) than the dark control samples. Following irradiation,
20 the base/neutral fraction had a lower proportion of pyridinic nitrogen (N₁) and a greater
21 proportion of N₁O_x classes, as shown in **Fig 4**. The prevalence of higher-order oxygen classes
22 indicated that multiple photochemical pathways exist for the oxidation of petroleum molecules.
23 Additionally, exposure to sunlight increased oil toxicity due to the increased water solubility of
24 the more polar oil photoproducts.
25
26

27 Ruddy et al⁹² investigated the molecular changes in oiled sands from Pensacola Beach
28 contaminated with Macondo well oil. To identify the primary environmental transformation
29 products of polar, high molecular weight (C>25) "heavy end" compounds that cannot be detected
30 by gas chromatography, this study employed FT-ICRMS with electrospray (ESI) and
31 atmospheric pressure photoionization (APPI) techniques. They observed that the petrogenic
32 material extracted from the Pensacola Beach sand had a molecular complexity that was twice as
33 high as the MWO constituents, particularly for oxygenated hydrocarbons.
34
35
36
37
38
39
40
41
42
43
44
45
46
47
48
49
50
51
52
53
54
55
56
57
58
59
60

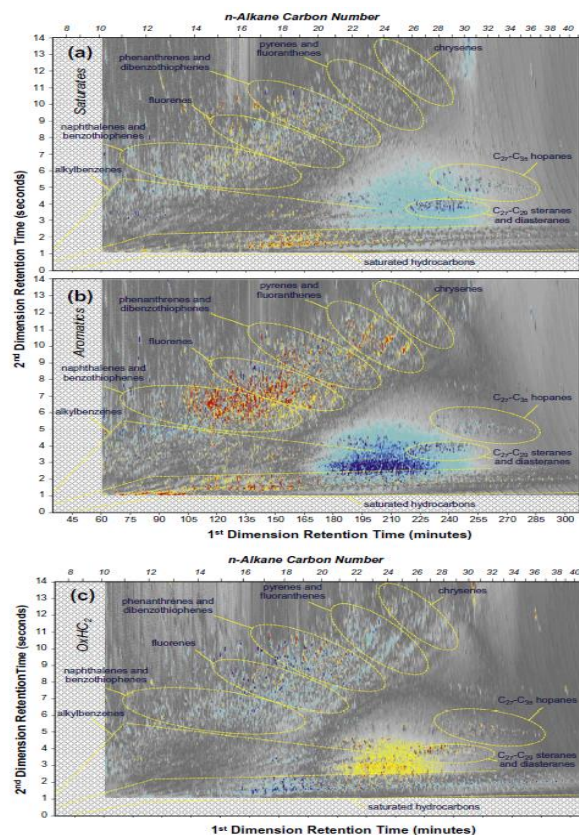


Fig. 3. PLS loadings for models predicting TLC-FID polar fractions from GCxGC-FID chromatograms (a) FSat (b) FAro and (c) OxHC₂. Blue peaks are negatively correlated with high concentrations of that fraction. Red and yellow peaks are positively correlated with those concentrations. For FSat this means that a peak that is persisting in weathered oil will appear as blue while peaks that are declining appear red. For OxHC₂ this means that a peak that is persisting in weathered oil will appear as red or yellow while peaks that are declining appear blue. “Peak heights” in loadings plots do not indicate large mass, but rather a strong correlation. Reprinted with permission from Hall et al.⁹¹

Both (±)ESI and (±)APPI ionization techniques detected a significant quantity of different oxygenated hydrocarbons in the Pensacola Beach sediment extracts. The notably high oxygen signal strength detected after using (+)ESI was ascribed to the conversion products of ketones (O₁ - O₈ classes), which matched the findings of a time-of-flight mass spectrometry (TOF-MS) investigation on model compounds. Carboxylic acid transformation products were observed in (-)ESI mode. The existence of high amounts of alkyl ketone fragments in sand extracts was unambiguously confirmed by using two-dimensional gas chromatography and FT-ICR-MS analysis, which disclosed the distribution of high-boiling ketone, carboxylic, and oxygen-containing transformation products with a higher number of carbons (3+). Additionally, GCxGC-FID analysis provided evidence that low boiling species had been removed from the light crude oil, and two-ring aromatics were decreased in abundance. Previously, an analysis of heavily weathered beach sand extracts using one-dimensional gas chromatography discovered a drop of 12 orders of magnitude in the ratio of relatively lighter (C₆-C₁₆) up to relatively heavier (C₁₆-C₃₅) alkanes.⁹³ The results broaden the range of oxygen-containing functional groups identified beyond the usual naphthenic acid type species to encompass a variety of complex and mixed classes, including ketones, alcohols, and carboxylic acids.

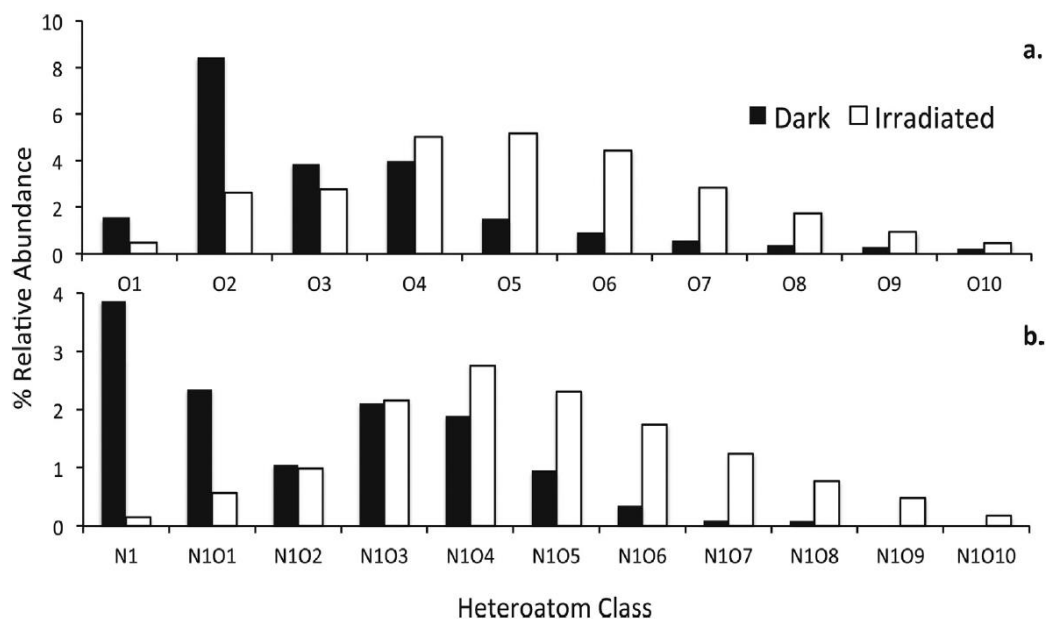


Fig. 4. (a) Negative mode ESI-FT-MS of acid fraction for the dark (black) vs. irradiated (white) samples modified with NH_4OH for the Ox series; (b) negative mode ESI-FT-MS of acid fraction for the dark (black) vs. irradiated (white) samples modified with NH_4OH for the N1Ox series. Relative abundance is normalized to all observed species for each sample. Reprinted with permission from Zito et al.⁵⁰

Roman et al.,⁹⁴ explored how photooxidation impacted the molecular content of seawater in the presence of both irradiated and non-irradiated oil slicks. The authors utilized ion mobility spectrometry-mass spectrometry (IMS-MS) and conducted analysis of PAHs under irradiated and non-irradiated oil slicks. The results showed that in the presence of irradiated oil, the seawater contained elevated levels of hydrocarbons along with byproducts containing oxygen and sulfur as compared to non-irradiated oil slicks. This study provided insights into the effects of photooxidation during a marine oil spill, designing replicated key elements of real-world conditions, including the use of freshly collected seawater, natural sunlight, and appropriate oil thickness and concentrations. Moreover, the results enhanced our comprehension of the fate and transport of a surface oil slick exposed to natural sunlight. Leveraging IMS-MS and PAH analyses provided an effective instrumental tool to characterize the chemical content of seawater within oil slicks, offering crucial insights for monitoring and evaluation of the consequences of oil spills on marine ecosystems. The study highlighted the importance of considering photooxidation as a factor influencing the fate and transportation of photoproducts during a marine oil spill, emphasizing the need for integrating realistic conditions in laboratory and bench-scale studies. It would be valuable to conduct experiments that incorporate a wider range of conditions and factors influencing oil photooxidation, such as different types and thicknesses of oil, variations in light spectrum and irradiance, and the impact of natural water flow patterns.

Lima, et al.⁹⁵ conducted a comprehensive study for 210 days to track the compositional changes in spilled oil over time under tropical climate conditions. Two different Brazilian oils A and B with 19 and 24 API respectively were studied under irradiated and non-irradiated conditions in a spill simulation experiment. According to the results obtained from FT-ICR MS, the oil samples that were exposed to solar irradiation produced oxygenated polar compounds. Additionally, it was observed that the abundance of *n*-alkanes and polycyclic hydrocarbons, such as

1
2
3 phenanthrene, dibenzothiophene, and chrysene, decreased significantly after 40 days under both
4 conditions. The authors stated that this decrease was due to evaporation. Furthermore, both oils
5 (A and B) experienced a considerable decrease in the levels of pristane and phytane isoprenoid
6 compounds, with the irradiated conditions showing a loss of 84% and 91% and non-irradiated
7 conditions showing a loss of 68% and 60% for oils A and B, respectively. Over the study period,
8 FT-ICR MS analysis of both oils revealed various modifications, such as a rise in the proportion
9 of compounds having more than two oxygen atoms (NO_3 , N_3O_3 , O_3 , O_4 , O_5 , O_4S , and O_5S) and a
10 decline in the proportion of classes like N_1 , NO , NO_2 , O_1 , and O_2 (as illustrated in Fig 5).
11 Conversely, the non-irradiated samples had a heteroatom distribution that matched the original
12 oils. Furthermore, the authors observed that the amount of O_3 compounds increased during the
13 spill simulation when exposed to sunlight, particularly as the carbon number range and double
14 bond efficiency (DBE) rose. Furthermore, there was an increase in the occurrence of compounds
15 with $\text{DBE} = 1$ in O_1 , O_2 , and O_3 categories, and compounds with $\text{DBE} = 2$ in O_3 and O_4
16 categories. These changes are consistent with other studies that observed photoproducts with
17 multiple oxygen atoms and with a range of DBE.
18
19
20

21 Another study on Macondo oil in the salt marsh sediments of Louisiana four years after the spill
22 was done by Chen, et al.⁹⁶ to detect the molecular composition of different compounds in
23 sediment samples using FT-ICR MS. The results showed the complexity and persistence of the
24 oxygenated compounds after 48 months from the spill. The incorporation of carboxylic acid into
25 the parent Macondo oil hydrocarbons in sediment extracts was detected, with an approximate 3-
26 fold increase in oxygen species after 9 months and reaching a peak of around 5.5-fold after 36
27 months, compared to the original parent Macondo oil hydrocarbons. The oxygenated species
28 with (O_4 – O_6) showed a relative increase in the abundance with time which was not found in the
29 parent compounds. The results showed that the most dramatic increase in relative abundance
30 during the 48 months post-spill period was in the mass of oxygen, which increased 7-fold after 9
31 months (3.9% by weight) compared to (0.5%), highlighting the complexity of oxygen containing
32 polar compounds. This change was attributed to oxidative transformation products as supported
33 by previous findings in other studies.^{91,97} Following 9 months of irradiation, 3% of the observed
34 compounds were moderately acidic species and 6% had one or more carboxylic acid groups.
35 There was also an increase in the proportion of carboxylic acids from ~ 8% to ~9% over 36 and
36 48 months, which could imply secondary oxidation. Carboxylic acids had the most abundant
37 proportion oxygen classes observed, followed by O_1 , O_3 , and O_4 . Differentiating between photo-
38 and biological oxidation in these complex systems is challenging.
39
40
41

42 Following the DWH oil spill, Aeppli, et al¹⁷ studied the weathering effect on oil-soaked sands,
43 surface slick, and boulders regarding the production of oxygenated species. An increase in
44 oxygenated fractions was detected in comparison to the aromatic and saturated fractions. This
45 rise in oxyhydrocarbons was attributed to carboxylation and hydroxylation, as evidenced by
46 FTIR results. The significant and dramatic changes in the oxygenated compounds happened in
47 the first three months after spill and later increased slowly. Furthermore, several long-chain
48 carboxylic acids C_{10} to C_{32} , as well as a variety of alcohols, were found in derivatized sand
49 patties according to GCxGC analysis, while these compounds were not observed in the Macondo
50 oil. The authors concluded that photooxidation and biodegradation share the role of production
51 of oxygenated compounds.
52
53
54
55
56
57
58
59
60

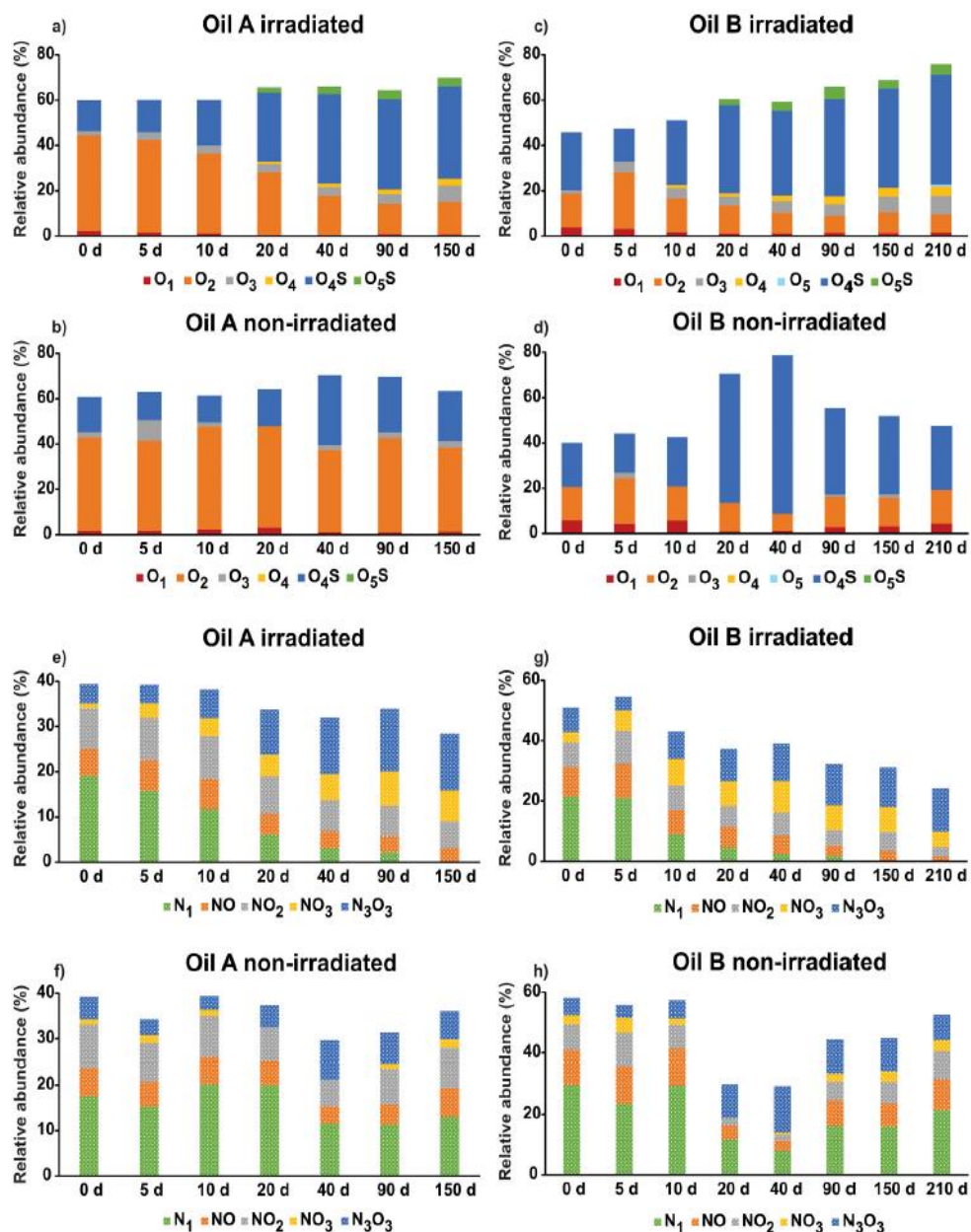


Fig. 5. Heteroatom class distribution obtained by ESI(-) FT-ICR MS for samples at 0 (original oil), 5, 10, 20, 40, 90, and 150 days for Oil A and Oil B at the same time plus 210 days, for both irradiated and non-irradiated units. Oxygenated classes are shown in a, b, c, and d, while nitrogen classes are shown in e, f, g, and h. Reprinted with permission from Lima et al.⁹⁵

The progression of oxidized, water soluble species from irradiated Macondo oil was studied by Zito et al.⁵⁹ According to the results, the photochemical oxidation of oil components produces surface-active, oil-soluble molecules. Dissolved organic matter hydrocarbons (DOM_{HC}) have the highest oxygen range, with species containing 1 to 18 oxygen atoms. Van Krevelen diagrams were utilized to detect the changes in the ratios of hydrogen to carbon versus oxygen to carbon for all identified species containing oxygen. This helped to demonstrate how highly oxygenated species move from the oil phase to the interface, and the aqueous phase. These findings are shown in Fig 6. As a result of having both polar and nonpolar functional groups, it is more probable for large molecules to remain in the interfacial region despite an increase in

oxygenation. When the O/C ratio of compounds exceeded 0.4, their solubility moved towards the aqueous phase. The distribution of photodegraded oil substances into the oil layer, the interfacial region, and the aqueous layer, resulting in dissolved organic matter of petroleum origin, was found to rely on the carbon number and oxygen content of the photoproducts. This observation provides a practical method for predicting the distribution of oil photodegradation products among these three phases and their transformation into petroleum-derived dissolved organic matter. In comparison to the dark control (3.3 mg C/L), the irradiated samples had substantial amounts of aqueous DOC (65.7 ± 4.8 mg C/L).

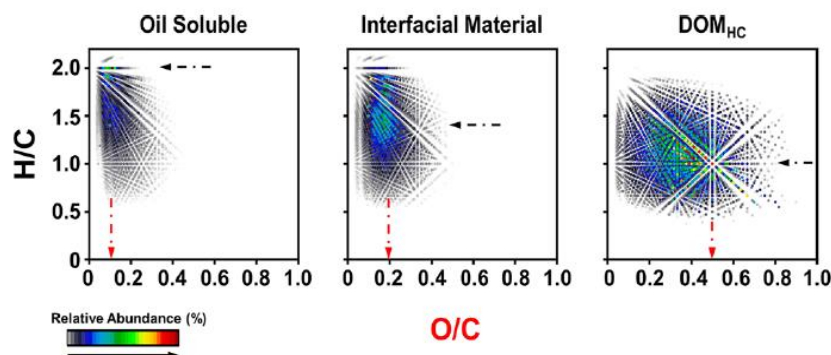


Fig.6. vK diagrams of the molecular formulae unique to each fraction shows the progression of higher oxygenated species from oil, IM, and DOM_{HC} fractions after simulated sunlight exposure. For each sample, black and red arrows highlight the most abundant H/C and O/C values, respectively. Reprinted with permission from Zito et al.⁵⁹

Generating of DOM_{HC} after photooxidation of different types of oil was also monitored by Whisenhunt et al.⁹⁸ In order to track the molecular properties of DOM_{HC}, the authors utilized three-dimensional fluorescence excitation-emission matrix spectroscopy (EEMs) and FT-ICR MS besides employing parallel factor and principal component analysis analysis to break down EEM spectra into individual components and assess the DOM_{HC} composition over time. The results indicated that refined fuels generated a considerably higher mass of photoproducts compared to crude oil. Optical analysis using EEMs revealed that the photooxidized, refined fuels had unique short-wavelength features, while crude oil decomposed into long-wavelength humic-like components and oxidized aliphatics, which is supported by FT-ICR MS data. Moreover, the authors stated that the composition of DOM_{HC} produced from different fuel types varied over time. The paper contributes to the understanding of photooxidized petroleum hydrocarbons in high latitudes and Arctic regions, offering potential applications in the early detection of oil spills. However, limitation of the research to a specific geographic region and high latitude conditions may limit the generalizability of the findings to other environments. The study demonstrated that molecular signatures of photooxidized petroleum varies as a function of petroleum refinement. The research did not directly address the potential ecological impacts of photooxidized petroleum hydrocarbons on marine ecosystems, highlighting the need for additional studies on marine biota toxicity.

Tarr et al.⁹⁹ stated that oil photooxidation is initiated by PAHs (chromophores) that absorb radiation in the solar spectrum and dominate oil photochemistry. Smaller PAHs degraded at a slower rate when exposed to sunlight compared to larger PAHs. This was because larger PAHs had a better match with the solar spectrum. On the other hand, the degradation of alkanes through photodegradation was much slower. The complex nature of the indirect photochemical reactions is not well understood, and additional mechanistic information is needed.

According to Ward et al.¹⁰⁰ the predominant source of oxygen that contributes to oil photooxidation is molecular oxygen rather than oxygen in water molecules. In addition, molecular oxygen exhibited a comparable kinetic isotope fractionation across various organic carbon varieties. For one week of irradiation, $\delta^{18}\text{O}$ contribution to oil increased from $-0.6 \pm 0.3\%$ (native oil) to $+7.2 \pm 1.1\%$. This 8-percentage point increase during transit to the coast was a minimum of 25-fold larger than the experimental error from extracted samples of the same deposited oil residue (0.3%). These findings showed that partial photooxidation, not biological degradation, was responsible for the attained shift in elemental and isotopic effect of the DWH oil. Although the role of molecular oxygen in photooxidation was clearly demonstrated, mechanistic and rate details are still unavailable.

Photooxidation and evaporation processes alter the physiochemical properties of the oil profile according to Ward et al.⁷⁹ The authors showed that with increasing exposure time, IR spectra (stretching of the carbonyl group) revealed an increase in oxygen concentration. Carbonyl group stretching intensity increased from less than 1% at the start of the irradiation to 3% after 24 hours. The physical properties of oil changed as well, with increasing of viscosity from 22 ± 1 to 147 ± 2 cP, density increasing from 0.88 to 0.92 g/mL, and adhesion increasing 6-fold from 0.09 to 0.55 mg mm². Generally, the photooxidation process changes the physiochemical properties of oil after a short term more than evaporation. However, oil spill models have not effectively incorporated these meaningful changes that are driven by solar exposure.

In terms of functionalization, several analytical investigations were concerned with the molecular transition after photooxidation. Cao and Tarr⁵⁵ applied MS/MS to monitor the production of aldehyde and ketones in a solar simulation study. Over the mass range of 200-1000 amu, about 80 aldehyde and ketone photoproducts were found. The detection of the 182 m/z fragment represents a typical fragmentation pattern for dinitrophenylhydrazine derivatized dicarbonyl, hydroxy carbonyl, and oxo-carboxylic acids as illustrated in Table 2. Furthermore, after solar irradiation, the amount of water-soluble organic compounds (WSO) in the samples increased. Use of high resolution mass spectrometry for analysis of these derivatized photoproducts would allow detection of lower concentration species as well as providing molecular formulas.

Ruddy et al,⁹² conducted a study using (+)ESI FT-ICR MS on spilled Macondo Well oil from Pensacola Beach to detect the oxidation photoproducts. According to the authors, it is probable that the positive ions observed as mono-oxygenated species were either alcohols or ketones. On the other hand, the negative ions observed as dioxygenated species were most likely carboxylic acids. The relative abundance of a ketone (4,4'-dimethylbenzophenone) being 10 times higher compared to a phenol (1-naphthol) at equal concentrations showed that ketones are much more effectively ionized by (+) ESI. The oxygenated species were separated through chromatography into four different fractions. The first fraction contained O₁-O₂ ketones, the second fraction contained O₁-O₅ species, the third fraction contained O₁-O₇ species, and the fourth fraction contained polyfunctional ketone/carboxylic acid species (O₁-O₈). Despite this and other publications providing some identification of functional groups present in photooxidation products, the composition of these materials remains minimally understood.

	Aldehydes	ketones	aromatic aldehydes	dicarbonyls	hydroxy-carbonyls	oxo-carboxylic acid	hydroxy-benzaldehydes
152	+++	+++	-	-	++	++	-
163	+++	+++	++	-	+	-	++
182	-	-	+++	+++	+++	+++	+++
[M-H-44]	-	-	-	-	-	++	-

Table 2. Common Fragment Ions in the MS/MS Spectra of Different Classes of Aldehyde- and Ketone-DNPH Derivatives Obtained by ESI-MS/MS. Adapted from Cao, Xian and Matthew A. Tarr.⁵⁵

Fathalla and Andersson⁶⁵ observed the presence of many carboxylic acids from (-) ESI MS/MS spectra of photooxidized Egyptian crude oil. Moreover, the authors observed the presence of cyclohexyl aromatics and certain fatty acids (C₄-C₁₆), which they attributed to the cleavage of the alkyl chain from polyaromatic sulfur hydrocarbons (PASHs) and terminal carbon oxidation. In addition, the mass spectrometry results revealed the existence of alcohols (diols and triols), as well as [M-15]⁺ ion and m/z 103 together, indicating the existence of fatty alcohols.¹⁰¹ The (-) ESI-MS/MS spectra showed the loss of the SO₃⁻ ion (m/z 80), which might be an indication for the presence of sulfonated aromatic compounds.¹⁰² Sulfobenzoic acids and carbonyl-containing compounds have been observed because of oxidation of alkyl groups or secondary oxidation opening the thiophene ring. No direct mechanistic evidence is available to verify the suspected pathways.

Niles et al.,⁵⁶ investigated the structural similarities of ketones/aldehydes in lab irradiated and field irradiated oil samples. The authors found that when oil was exposed to simulated solar irradiation, the photooxidation was the primary pathway for creating aldehydes and ketones. The (+) ESI FT-ICR MS spectra showed the abundance of O_x classes in field samples and laboratory irradiated samples compared to the dark control. Meanwhile, field samples showed a higher abundance of O_x species than the laboratory irradiated sample. In addition, there was a significant variation in the way carbon atoms were spread out between samples that had been irradiated in a laboratory and had low numbers of carbon atoms (as low as C₁₂ for O₁), and samples collected from the field that did not have any low carbon number species. Such comparison of field and lab results are important, but additional correlations are needed to translate lab results to field modeling.

Indirect photolysis produces a variety of reactive transition species such as hydroxyl radical and singlet oxygen.¹⁰³ Tarr's research group studied the production and effects of organic triplets, hydroxyl radicals, and singlet oxygen on dissolved organic matter (DOM) after photooxidation in three different studies. Zito and Tarr⁵¹ studied the creation of hydroxyl radical in samples collected after the DWH oil spill using benzoic acid as a probe over seawater and pure water. The results showed that the production of hydroxyl radicals participate in the fate of spilled oil. The amount of trapped hydroxyl radicals in Gulf of Mexico water was 33% lower on average than in pure water. In another investigation, Zito and Tarr⁴⁹ studied the production of singlet oxygen from oil films over seawater and pure water using furfuryl alcohol as a chemical probe. The amount of singlet oxygen produced for oil on pure water was 1000 times higher than the amount created for oil on sweater. Within the time frame of this study, seawater samples without oil produced very little ¹O₂, indicating that the primary source of created singlet oxygen is oil photochemistry. Because the probes used in these studies were water soluble, the trapping was predominantly in the aqueous phase and did not directly measure formation in the oil layer.

Zito and Tarr,⁴⁸ in other work observed the generation of excited triplet states during photochemical oxidation of petroleum in Gulf of Mexico water and pure water, with no significant differences between the two matrices. The transformation of *cis*-pentadiene isomer to *trans*-pentadiene was brought about by energy transferred from the excited triplets formed in the oil during irradiation. A photostationary state (PSS) was attained in around 5 hours, which is

about 12 times faster than in a prior work on DOM by Zepp et al.¹⁰⁴ The triplet states produced in petroleum samples were with energies more than 280 kJ/mol in all cases, demonstrating that the petroleum precursors could generate high-energy triplet states. The chemistry of these excited states and their energy transfer properties has not been studied in oil or water.

Using Paper spray ionization mass spectrometry (PSI-MS) to estimate the degree of photodegradation of spilled oil, Kim et al.,¹⁰⁵ showed that more oxidized compounds containing sulfur such as O_5S_1 and O_6S_1 increased, whereas less oxidized species decreased. Further observations of the oxygenated sulfur compounds revealed that their concentration increased in both laboratory photodegraded and naturally degraded oil samples in alignment with previous reports¹⁰⁶ (Fig.7). To better comprehend these chemical alterations, it was discovered that the O_5S_1 and O_6S_1 compound classes have a 5 to 40 carbon number range and DBE values ranging from 0 to 10, with the O_6S_1 class having a higher DBE distribution than the O_5S_1 class. The authors attributed the increase in DBE to the development of functionalized oxygen groups such as carbonyl, carboxyl, and hydroxyl groups. This report is among several that have shown oxygenation across heteroatomic species.

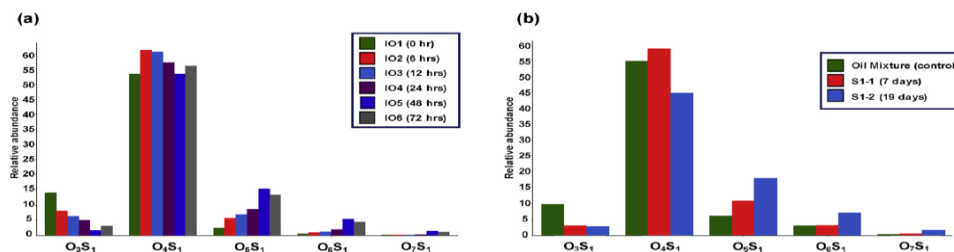


Fig. 7. Comparison of major class distribution of (a) photo-oxidized IHC samples and (b) spilled oil samples obtained in negative ion mode PSI. Reprinted with permission from Kim et al.¹⁰⁵

Griffiths et al.,⁴⁶ using API-FTICR MS, demonstrated that among the complex mixture, chemicals containing sulfur or nitrogen were reactive under radiation. According to the authors, compositions with higher DBE were mainly unaffected due to the high photostability of their conjugated systems, whereas structures with a smaller number of DBE were more reactive. Furthermore, photooxidation of pyrrolic nitrogen-containing compounds was easier than photooxidation of pyridinic nitrogen-containing compounds. The reactivities of various compounds corresponded with the compound class and DBE during the five-week irradiation period, rather than carbon number. Naphthenic acids were found to be the most common photooxidized products. Such products represent a potential increase crude oil toxicity after subjection to sunlight. Similar results were obtained by Zito et al.,⁵⁰ as after oil irradiation there was a depletion in the quantity of pyridinic nitrogen (N_1) and an increase in N_1O_x classes abundance in the base/neutral fraction. In the dark water soluble organic fraction (WSO), N_1O_1 species were similarly common, with a relative abundance of 2.3%. However, in the irradiated WSOs, N_1O_4 were the highly abundant nitrogen species observed in negative-ion mode. The fact that N_1O_5 - N_1O_7 species have a broad range of DBE and carbon numbers, and their relative abundance increases after exposure to radiation, suggested that the oxidation process occurs in multiple phases. After irradiation, it was observed that nitrogen-containing species belonging to the N_1O_x classes exhibited multiple oxygen atoms per molecule. This indicated that nitrogen-containing species with basic properties are susceptible to undergoing several oxidation reactions.

1
2
3 King et al,⁵⁷ conducted a broad investigation to study the effects of the photochemical reactions
4 on the weathered DWH oil collected from oil slicks on the GoM surface and exposed
5 subsequently to simulated solar irradiation. Small losses of alkanes were recorded, meanwhile a
6 noticeable PAH degradation was detected. When the weathered oil was exposed to simulated
7 sunlight for 5 days, roughly 80% of the PAH content was lost. The weathered oil samples
8 showed no noticeable quantities of molecules with less than C₁₃, according to GC data, likely
9 due to evaporation and dissolution prior to sample collection from the sea surface. Moreover,
10 monocyclic aromatics were mainly absent, however bicyclic aromatic hydrocarbons were present
11 at concentrations relatively low in comparison to other PAHs, according to fluorescence data.
12 The concentration of alkanes with higher molecular weight, such as C₁₉, C₂₀, C₂₂, C₂₃, and C₂₈,
13 reduced by 5% after irradiation for 3 hours, equivalent to 0.63 days of sunlight, and by 20% after
14 a 48-hour irradiation period, equivalent to 10 days of sunlight. Within the exposure time, there
15 was a depletion in degradation rate, which could be due to the photobleaching of sensitizers.
16 While this study revealed some time-dependent trends, the intricate behavior across the complex
17 mixture was not elucidated.
18
19
20

21 Islam et al,⁴ studied the structure-dependent degradation of polar compounds in weathered oil.
22 The samples examined in this study were collected from stages II and IV from the site of the
23 M/V Hebei Spirit oil spill and a fresh mixture of the same oils from the same accident. The
24 results of the mass spectrometry analysis using atmospheric pressure photo-ionization and
25 hydrogen/deuterium exchange technique indicated that the presence of oxygen-containing
26 compounds increased the production of [N₁O₁+H]⁺, [N₁O₁+D]⁺, [S₁O₁+H]⁺, and [S₁O₁+D]⁺ ions.
27 Additionally, the concentrations of these compounds also increased as the weathering process
28 progressed.^{50,107} Moreover, [N₁O₁+H]⁺, [N₁O₁+D]⁺ ions recorded changes across all DBE ranges.
29 Significant increase of [S₁O₁+H]⁺ ion and [S₁O₁+D]⁺ ion with high DBE were recorded in the
30 fresh oil mixture in comparison to the naturally weathered oil samples collected from both
31 stages. The results demonstrated that secondary and tertiary amines were more vulnerable to
32 photo-degradation than compounds containing pyridine, suggesting structure-dependent
33 degradation of polar compounds in weathered oils.
34
35
36

37 Neuman et al,¹⁰⁸ studied the production of ozone and alkyl nitrate (RONO₂) through
38 photochemical reactions when evaporated hydrocarbons interacted with NO_x emissions (NO +
39 NO₂) resulting from spill response activities. The study focused on the reaction of NO_x present in
40 the maritime environment due to ship exhaust and the atmosphere located in the downwind
41 direction of the DWH oil spill. The obtained measurements in the study were collected on 8-10
42 June 2010 in the area surrounding the DWH spill at altitudes between 60 and 200 m above the
43 Gulf of Mexico. The samples showed concentration of C₅–C₁₀ alkanes greater than 10 ppbv.
44 These detected concentrations were greater than in U.S. urban and industrial areas.¹⁰⁹ The
45 authors mentioned that the high OH loss rates were caused by alkanes scavengers. Meanwhile,
46 NO₂, CO, CH₄, and alkenes contributed only a modest amount to the OH loss rate. Moreover, the
47 presence of high alkane amount resulted in the rapid formation of O₃, but the production of
48 RONO₂ through radical termination reduced the O₃ yield. The photochemical behavior of
49 volatile oil compounds from the DWH spill was not well studied, and volatile photoproducts
50 from irradiated oil have not been characterized.
51
52
53

54 The reviewed articles demonstrated substantial advances in oil photoproduct detection through
55 employing a diverse array of analytical techniques. The complexity of oil and irradiated oil poses
56 challenges for their analysis. Clearly demonstrated from studies on Macondo oil photochemistry
57
58
59
60

1
2
3 is that a range of oxygenated photoproducts is produced, likely involving the full composition of
4 the oil. The complex mixture of photoproducts impacts the physical, chemical, and biological
5 behavior of the sunlight-weathered oil. Mechanistically, the participation of PAHs in direct and
6 indirect photolysis is evident, although the details of indirect photolysis are lacking. Multiple
7 reactive transients are involved, allowing the reaction of saturated as well as aromatic
8 compounds. Oxygenation is predominantly through reaction with O₂, thus making exposure to
9 the atmosphere a critical factor in oil photodegradation. Details that have not been clarified
10 include the mechanisms of photochemistry in the oil phase and the role and progression of
11 secondary photochemical reactions in the aqueous phase. Over time, irradiated oil and its
12 photoproducts become increasingly oxygenated, resulting in a distribution of photoproducts
13 across the oil, oil-water interface, water, and perhaps other compartments (e.g., oil-air, water-
14 particulate). Notably absent from the studies on the photochemistry of Deepwater Horizon oil as
15 well as other oil spills is the investigation of gas-phase photoproducts. Oxidation of heteroatoms
16 has also not been effectively studied, and the role of chelated metals in the photochemical
17 mechanisms (as chromophore and/or reactant) is also not understood.
18
19
20

21 *Connections between photochemistry and biological systems*

22
23 As oil is exposed to sunlight, it becomes oxygenated, making it more polar, more water-soluble,
24 and thus more bioavailable. While these changes may make the photoproducts more amenable to
25 biodegradation through endogenous microflora, with increased bioavailability also comes a
26 potential increase in toxicity. Though both the biodegradation and toxicity of crude oil
27 photoproducts remain poorly investigated, the few studies concerned with them demonstrate that
28 there are connections worth exploring further.
29

30 Colonies of the marine bacterium *Aliivibrio fischeri* are frequently employed to monitor the
31 toxicity of aqueous compounds as part of the Microtox® analysis method.¹¹⁰ A noticeable
32 decrease in the bioluminescence of this bacterium upon addition of the sample compared to a
33 negative control can be attributed to an increase of toxicity in the aqueous environment. This
34 method was employed by King et al.,⁵⁷ as for the first time to investigate the toxic effects of
35 solar-exposed oil from the DWH spill using oil and water collected about 47 miles from the spill
36 site on May 26, 2010. The authors found that an increase in irradiation time resulted in a
37 significant increase in the water's toxicity, reaching about 85% inhibition after 25 h of
38 irradiation, suggesting a link between the toxicity and increasing water solubility of the
39 photoproducts. No toxicity was associated with the dark control sample, which was credited to
40 the oil having already been depleted of water-soluble compounds after traveling through the
41 water column from the source of the DWH leak to the surface. The use of *A. fischeri* is relevant
42 to marine systems, but it does not provide data on toxicity to other species, including different
43 bacterial species.
44
45
46

47 Building on these initial results, King et al.⁵⁸ expanded their research in another study using the
48 same oil as they did previously but this time adding TiO₂ or Fe₂O₃ as photocatalysts before
49 irradiation. Irradiation times ranged from 3 to 24 hours, with a dark control being run for each
50 sample type. After irradiation, the aqueous fraction was separated for the toxicity assessment.
51 While all three sample types (no photocatalyst, TiO₂, Fe₂O₃) showed a strong increasing trend in
52 toxicity as the irradiation time was increased, the samples with either photocatalyst were deemed
53 less toxic than the sample without any added oxide for irradiation times of 3 and 6 hours. After
54 12 hours of irradiation, the photocatalyst samples became more toxic, though all three groups
55
56
57

1
2
3 reached a similar level of toxicity after an irradiation time of 24 hours, each inhibiting between
4 80 and 90% of bacteria. These results indicated that continued photodegradation of oil may yield
5 compounds that are more toxic. While photocatalyst use in marine systems is currently
6 impractical, changes in product toxicity indicate that different photochemical mechanisms result
7 in different impacts.
8

9
10 The toxicity of oil photoproducts was further examined by Zito et al,¹¹¹ also utilizing Microtox®.
11 After irradiating films of light (Macondo well) and heavy (NIST 1621e) oil over seawater for up
12 to 240 h, the aqueous phase containing the dissolved organic matter (DOM) was collected and
13 filtered using 0.27 µm glass microfiber filters and the pH adjusted to 7. Prior to Microtox®
14 testing, the DOM samples were carbon normalized to determine the toxicity not as a function of
15 the concentration but composition of the sample. Microtox® testing showed that the acute
16 toxicity per unit carbon decreased as irradiation time was increased and more DOM was
17 produced. Maximum toxicity per unit carbon was found to occur after 24 h of irradiation
18 (corresponding to about 1 week in the natural environment) for both light and heavy oil DOM,
19 with 62% and 54% toxicity, respectively. Afterward, the toxicity per unit carbon decreased
20 steadily for both DOM types. The heavy DOM eventually reached 0% toxicity per unit carbon
21 after about 168 h, while the light DOM remained at about 12% toxicity per unit carbon after 120
22 h of irradiation. A Spearman rank correlation of data from FT-ICR-MS analysis compared to the
23 toxicity per unit carbon for all DOM samples confirmed that the compounds produced early
24 during irradiation were the most toxic and became less toxic as they were oxidized. Nevertheless,
25 the overall toxicity of a sample may still increase as the amount of DOM builds up over time,
26 even if the toxicity per unit carbon decreases. Additional time-dependent toxicity studies with
27 other organisms would provide a richer understanding of the transient nature of photoproduct
28 toxicity.
29
30
31

32 A different method for the determination of oil photoproduct toxicity was explored by Kim et
33 al.,¹¹² who irradiated diesel oil and seawater collected from a spill in Jangmok Bay, Korea in 2 L
34 glass bottles by placing them on a rooftop for five days, with a seawater sample being collected
35 each day via a stopcock at the bottom of each bottle, and then used artificially fertilized olive
36 flounder (*Paralichthys olivaceus*) eggs to determine possible toxic effects. After fertilization, the
37 eggs were incubated at 16°C in the dark with pure seawater or seawater with photoproducts. The
38 embryos were examined under a stereomicroscope or compound microscope after 48 h of
39 exposure. In addition to increased mortality, three other frequent effects were observed for which
40 the frequency was calculated: Pericardial edema (PE), dorsal curvature (DC), and tailfin defects
41 (TF). While the mortality rate of embryos exposed to non-irradiated oil was 20%, exposure to oil
42 that had been irradiated for two days increased to 64% and, after five days of irradiation, 100%.
43 The patterns of the other three parameters were analogous, with PE reaching a roughly 100%
44 frequency after a single day of irradiation, and both DC and TF following suit after two days. (–)
45 ESI FT-ICR MS analysis of the aqueous fraction of the samples showed that O₃ and O₄ class
46 photoproducts became much more abundant with increased irradiation, indicating a link between
47 those compounds and developmental toxicity. Partial least-squares regression was used to
48 construct a model to predict toxicity, which confirmed that more polar compounds contribute to
49 an increase in toxicity. While photoproducts clearly demonstrated toxic and deforming impacts,
50 it is unclear how prevalent these impacts would be in real systems where dilution of
51 photoproducts in seawater is likely.
52
53
54
55
56
57
58
59
60

1
2
3 Harriman et al.¹¹³ monitored the respiration of native Gulf of Mexico microbial communities
4 exposed to sand patties. Sand patties and un-oiled sediment were collected from Gulf Shores and
5 Fort Morgan, AL on January 20, and March 18, 2014. For the assessment of aerobic respiration,
6 triplicate incubations were prepared with Gulf of Mexico sediment inoculum and sterilized
7 seawater, and O₂ uptake was measured over 3 days using a respirometer. For anaerobic
8 respiration, varying ratios of sediment and crumbled sand-patty were added to 120 mL bottles
9 with 10 mL N₂-bubbled seawater and 50 nCi ³⁵SO₄²⁻ under an 80:20 N₂:CO₂ headspace and
10 compared to a control using only endogenous inoculum. After 7 days of incubation at room
11 temperature, the H₂³⁵S generated by the microbes was volatilized, then trapped for scintillation
12 counting. When analyzing the respirometer data concerning both the sulfide production and O₂
13 consumption, the authors found that the addition of sand-patty derived DOM did not result in a
14 decrease in respiration of the microflora, but rather it remained the same or even resulted in an
15 increase, thereby indicating that the sand patty components are not toxic to the local Gulf of
16 Mexico microflora but may stimulate microbial respiration and undergo biodegradation. To
17 further investigate, sand patties were sliced, crumbled into sterilized seawater, and irradiated for
18 increments of 3 or 12 h at a time using an Atlas CPS+ solar simulator for a total of up to 84 h,
19 with the seawater and DOM being removed after each irradiation increment and replaced with
20 fresh sterile seawater. Gulf of Mexico sediment inoculum and sand-patty derived DOM from
21 either irradiation procedure or the dark control were then added to 250 mL bottles and analyzed
22 by the respirometer for O₂ every 4 h for a total incubation time of up to 68 h. The rates of O₂
23 utilization were compared to each other and to a sterile negative control. After 68 h incubation
24 time, the endogenous control microflora had respired about 38 μM O₂, the inoculum using whole
25 sand patties about 64 μM, the dark control 67 μM, and the sample using photosolubilized DOM
26 about 114 μM total. This indicated that the DOC was much more susceptible to aerobic
27 biodegradation after being irradiated. This study demonstrates that diverse microbial
28 communities can thrive rather than suffer toxicity due to oil photoproduct exposure.
29
30
31
32
33

34 Also using respirometry as a means to measure biodegradability of oil photoproducts in their
35 study, Brame et al.⁸³ collected DWH oil from Barataria Bay, LA, in October 2010 and irradiated
36 it in ultrapure water with 0.5 wt. % food-grade TiO₂ (FG-TiO₂) in a Philips TL4W photoreactor
37 for 24 h on a stir plate. Another set of samples was irradiated naturally for 11 days in glass jars
38 on orbital shakers. As these latter samples were uncovered, water was replenished twice daily.
39 Dark controls and no catalyst controls were run, as well as no oil controls to determine the
40 production of reactive oxygen species (ROS) without oil. The authors found that O₂ consumption
41 in both artificially irradiated groups with and without the FG-TiO₂ photocatalyst initially showed
42 a steep increase, both having utilized about 9 mg of O₂ after 25 h, while the dark control
43 consumed little to no O₂ in that same timeframe. During the following 100 h of respirometry
44 tests, the group treated with FG-TiO₂ consumed an additional 6 mg O₂, while the irradiated
45 group without photocatalyst consumed only another 2 mg and the dark control about 1 mg. Both
46 groups irradiated under natural sunlight with and without FG-TiO₂ showed an identical pattern
47 during the first 25 h of respirometry analysis, also consuming around 9 mg of O₂ in that initial
48 timeframe. However, unlike the groups irradiated in the laboratory, neither consumed any further
49 significant amount of O₂ after this timepoint until measurements were concluded after 40 h.
50 DOC analysis of the naturally irradiated samples showed that, unlike in the artificially irradiated
51 samples, the addition of FG-TiO₂ had not resulted in a significant increase in DOC compared to
52 the samples without it. The authors ruled out insufficient irradiation as a cause as the
53 measurements revealed that samples without oil but with FG-TiO₂ generated ROS even under
54
55
56
57
58
59
60

1
2
3 natural sunlight. Instead, they suggested that the lack of increase in DOC could be due to the
4 different mixing methods of the orbital shaker employed for those samples, which may have
5 caused the FG-TiO₂ to sink to the bottom of the containers where the ROS it generated could not
6 react with the oil. Assuming the measured O₂ consumption to be directly related to the rate of
7 biodegradation, the authors concluded that the addition of a photocatalyst such as FG-TiO₂ could
8 increase the biodegradation of oil exposed to sunlight due to the larger amount of DOC
9 generated in the presence of the catalyst. However, they noted that the catalyst may need to be
10 modified to possess greater buoyancy or hydrophobicity for it to remain close enough to the oil
11 floating on the surface in a natural environment.
12
13

14 In a different approach, Bacosa et al.⁶⁸ examined biodegradation by directly monitoring the of
15 concentration of alkanes, PAHs, and alkylated PAHs with increasing exposure to sunlight and
16 comparing it to the measured concentration loss due to photodegradation. Three treatments each
17 of dark and light incubations were prepared. The samples were light Louisiana sweet crude oil
18 (LLS) with seawater collected from the DWH oil spill site in May 2013 with and without the
19 addition of the dispersant Corexit 9500A, and the control consisted of LLS with seawater. An
20 equivalent dark control was run for each of the three categories. The light incubations were
21 subjected to the natural daylight cycles aboard the *R/V Pelican* and later at the Pier Laboratory of
22 the University of Texas in an incubator with running surface water for up to 45 days, with
23 samples being taken in triplicate on days 0, 5, 10, 20, 27, and 36. It was found that *n*-alkanes (C₉-
24 C₃₇) in both the dark and the light oil incubation degraded faster with dispersant than without, as
25 *n*-alkanes in both light and dark oil treatments without the dispersant experienced major
26 degradation only after a lag of about 10 days. A clear difference could be seen between the
27 irradiated and dark control, the latter of which did not exhibit significant degradation of *n*-
28 alkanes, indicating that the decrease of the *n*-alkane concentration in the irradiated control (about
29 30%) was caused by photooxidation, not biodegradation. Pristane and phytane, on the other
30 hand, did not seem to degrade as much when irradiated, only losing a fraction of their initial
31 concentration, while the dark samples degraded completely after about 45 days. The authors
32 suggested that this may be due to the inhibition of the bacteria responsible for the biodegradation
33 of pristane through UV irradiation. After computing the rate constants, the authors concluded
34 that biodegradation played a major role in the degradation of alkanes, with a shorter chain length
35 (*n*-C₉ to *n*-C₁₃ for dark, *n*-C₉ to *n*-C₁₄ for light) corresponding to an increased rate constant, and
36 that the use of Corexit 9500A enhanced the biodegradation of these shorter chains. In the
37 disappearance of PAHs, in contrast, photooxidation seemed to be more prominent. While the
38 dark control showed no changes, the dark treatments with and without dispersant began
39 degrading only after a lag of 5 and 10 days, respectively, and about 10% of the initial
40 concentration remained from about 27 days until the experiment concluded. All light treatments,
41 including the control, had complete degradation after about 36 days. Further analysis showed
42 that 3-ring PAHs were more easily photo-oxidized than 4- or 5-ring PAHs, which contradicted
43 earlier studies using simulated sunlight.^{58,114} An analysis of the dark treatments indicated that
44 naphthalene was the most easily biodegradable PAH, with a lag period of about 5 days, and
45 phenanthrene second, with a 10-day lag. A similar degradation pattern for each treatment was
46 observed for alkylated PAHs, though no pattern regarding the ring numbers could be determined.
47 Overall, the authors concluded that biodegradation was likely outpaced by photooxidation in the
48 disappearance of PAHs and alkylated PAHs under the conditions of the study. The
49 interdependence of photochemistry and biodegradation requires further study to be clarified.
50
51
52
53
54
55
56
57
58
59
60

1
2
3 Bacosa et al.¹¹⁵ also identified specific bacterial genera that are influenced by sunlight in the
4 presence of spilled oil. Sunlight significantly reduced bacterial diversity and shifted community
5 structure. Further research is needed on the interplay of crude oil, dispersant, sunlight, and other
6 factors to properly assess the biodegradation capacity of a system. While the study provided
7 valuable insights into the role of sunlight in shaping bacterial communities in oil-polluted surface
8 waters, it was restricted to Gulf of Mexico water and may not be representative of other marine
9 environments or regions with different conditions. The study also did not investigate the long-
10 term effects of sunlight on bacterial communities, the potential for microbial adaptation over
11 time, or the specific mechanisms by which sunlight influences bacterial community composition
12 and dynamics in the presence of oil and/or dispersant. All of these limitations highlight the need
13 for further research to better understand the underlying mechanisms involved.
14
15

16
17 In their study to explore the effect of photooxidation on the molecular structure of seawater in
18 the presence of both irradiated and non-irradiated oil slicks using IMS-MS, Roman et al.,⁹⁴ also
19 employed biomimetic extraction (BE) to measure both neutral and ionized components in the
20 seawater samples and then utilized these BE measurements to calculate toxic units (TU) as a
21 means of assessing the potential aquatic risk. The automated analysis of BE with solid phase
22 microextraction was conducted using gas chromatography equipped with a flame ionization
23 detector. The BE collected data showed that the TU in irradiated mesocosms experienced an
24 elevation, primarily driven by ionized components. Nonetheless, these TU values stayed below
25 1, indicating a limited potential for ecotoxicity. Furthermore, the quantified PAHs in the water
26 analysis accounted for a relatively small portion of the overall TU associated with the neutral
27 dissolved constituents, ranging from 0.1 to 2.7 in non-irradiated conditions and 9.0 to 12.7 in
28 irradiated conditions. The bioavailability of neutral and ionized acid extractable organic acids
29 evaluated by SPME demonstrated an overall rise in total TU when exposed to sunlight. The
30 approach applied in this study enabled the combination of BE and TU calculations which serves
31 as a valuable tool for appraising the potential environmental risk associated with oil
32 photooxidation, which aids in the evaluation of the ecotoxicity of spills. However, applying the
33 biomimetic extraction BE and APPI showed some limitation in identifying the toxicity of
34 particular analytes and to gauge the possible environmental risks associated with the exposures.
35
36
37

38 With only a few published reports, the interplay between biological and photochemical process
39 for sunlight exposed DWH oil is poorly understood. Clearly demonstrated is that sunlight
40 exposure can increase water solubility, biodegradability, and toxicity. Studies that utilized
41 Microtox showed acute toxicity, while fish embryo studies demonstrated severe developmental
42 inhibition. However, the mechanisms (including identity of the active chemical agents) of
43 toxicity and potential genotoxicity have not been uncovered. Furthermore, an understanding of
44 the behavior of toxic and genotoxic photoproducts in the environment does not exist. Impacts of
45 oil photoproducts on individual species do not demonstrate ecosystem response, and work with a
46 microbiome (as opposed to a single species) has demonstrated that overall microbial growth can
47 be stimulated despite the presence of toxic photoproducts. Dilution of photoproducts in a real
48 system has also not been effectively addressed in existing reports from laboratory studies.
49 Studies on the genotoxicity of oil photoproducts are also lacking.
50
51

52 **Analytical techniques used to monitor photoproducts**

53 While oil analysis has been extensively studied, this section reviews the techniques that were
54 specifically applied to the analysis of oil photoproducts. Improved analytical success can be
55
56
57

1
2
3 achieved by integrating multiple analytical approaches, including hybrid analytical platforms.
4 Much progress has been made in this area over the previous few decades.⁵⁹ The advances in
5 petroleum analysis has paralleled advances in ionization techniques and mass spectroscopy
6 analysis. ESI was first established in 1990 by Fenn et al¹¹⁶ but was combined with low-resolution
7 MS. Later, ESI was applied with advanced high-resolution MS such as FTICR MS making
8 molecular level characterization possible. The complexity of oil increases after weathering
9 processes resulting in even greater challenges for its characterization and furthering the necessity
10 for these high-resolution techniques. Throughout the weathering processes, new compounds are
11 formed with different chemical and physical properties compared to the parent compounds. Due
12 to their greater-water solubility and hence ability for fast dispersion in marine systems,
13 compounds with enhanced polarity represent the highest threats.¹¹⁷ Therefore, it is crucial to
14 perform a thorough analysis at the molecular level of both the polar compounds and their
15 nonpolar precursor compounds, in order to identify the changes that take place over time. Since
16 the topic of this review is oil photochemistry, the analytical techniques mentioned in this section
17 are limited to studies of photoproducts after oil exposure to sunlight or simulated sunlight.
18
19
20

21 *Fourier Transform Ion Cyclotron Resonance Mass Spectrometry (FT-ICR MS)*

22
23 FT-ICR MS is a frequently applied technique for weathered oil characterization and forensic
24 investigations due to its high resolution and accuracy.¹¹⁸ The carbon number diversity of fossil
25 hydrocarbons was previously reported to be from C₁ to about C₁₀₀.^{119,120} Various ionization
26 techniques, such as ESI and photoionization (APPI) have been employed, combined with FT-
27 ICR MS, to analyze oil photoproducts. McKenna et al.¹²¹ conducted a study using FT-ICR MS to
28 analyze the molecular properties of petroleum from the Macondo well. The petroleum was
29 collected from a tar ball found on a beach in Louisiana. Their aim was to determine the initial
30 composition of the material that was released into the Gulf of Mexico after the DWH oil spill. To
31 widen the spectrum of analysis of neutral and acidic species in crude oil and improve the
32 ionization efficiency of weak acids, ESI was utilized in the presence of tetramethylammonium
33 hydroxide. The findings indicated that the crude oil extracted from the Macondo well had over
34 30,000 molecular compositions, including acidic, basic, and nonpolar compounds. These
35 advances were crucial since oil photoproducts are even more complex than the initial oil.
36
37

38 **Fig. 8** shows the compositional window that can be accessed by several methods. Due to its
39 narrow window, GC cannot resolve the complexity of crude oil. The GCxGC range shown in
40 Fig. 8b represents complete chromatographic resolution from C₈ to C₄₂ alkanes.¹⁴ While GCxGC
41 can access this range, it is not possible to separate petroleum compounds with more than thirty
42 carbons due to the vast number of potential structures and the resulting complexity.^{122,123} A wide
43 range of hydrocarbons released from the DWH accident are out of the range of GC and even
44 GCxGC. The analytical window for GC, GCxGC, and the extension to C₁₀₀ is illustrated in Fig.
45 8c, which demonstrates the compositional coverage attainable by using a combination approach
46 and the degree of overlap between them. Fig. 8d represents more complete analytical coverage
47 from C₈ to C₁₀₀ through a combination of methods.¹²⁴ Because of the complexity and range of
48 sizes and polarities of oil photoproducts, effective analysis requires a combined instrumental
49 approach.
50
51
52

53 Using of ESI and APPI combined with FT-ICR MS, Ruddy et al⁹² conducted a comparative
54 analysis of hydrocarbon molecules presented in oiled sands from Pensacola Beach and Macondo
55 wellhead oil. They identified significant environmental transformation products that were high
56
57
58
59
60

1
2
3 molecular weight ($C > 25$). Corilo et al¹²⁵ conducted a fingerprint study to determine the source of
4 heavy fuel oil that was spilled from two ruptured tanks on the motor vessel Cosco Busan after it
5 collided with the San Francisco-Oakland Bay Bridge in November 2007. They used principal
6 component analysis to determine the relative abundances of component classes N, NO, NS, and
7 O₂ species identified as potential indicators for seven weathered samples obtained from the
8 Cosco Busan spill site. As the duration of weathered exposure increased, there was a decrease in
9 the proportion of compounds that had only one nitrogen atom (N₁), while the proportion of
10 compounds with multiple heteroatoms and oxygen (NO, O₂) increased. The relative abundance
11 of NS species, on the other hand, remained constant until day 511, implying that it might be used
12 as an internal marker.
13
14

15 Griffiths et al⁴⁶ used APPI combined with FT-ICR MS to assess the changes in the composition
16 of crude oil following simulated exposure to solar radiation. The authors also incorporated data
17 from negative-ion and positive-ion ESI to support their findings. The study utilized APPI
18 combined with FTICR MS due to its capability to ionize a wide range of compounds, including
19 those with low polarity that could not be analyzed by ESI.^{126,127} Moreover, APPI was chosen for
20 its ability to generate both radical cations and protonated ions from the same sample through
21 separate pathways. Furthermore, for determining these less polar compounds, APPI does not
22 require any derivatization.^{128,129} In work on DWH oil photooxidation, Zito et al. conducted two
23 studies focusing on the generation of oxygenated species. The first study involved the extraction
24 of water-soluble organics (WSO) from Macondo well oil samples that were either kept in the
25 dark or subject to irradiation, followed by analysis with FT-ICR MS.⁵⁰ Liquid-liquid extraction
26 was performed to separate the samples into two fractions: acidic WSOs that could be analyzed
27 using negative-ion ESI, and base/neutral WSOs that could be analyzed using positive-ion ESI.
28 These fractions were then analyzed with FT-ICR MS to identify the molecular changes that
29 occurred in the WSOs due to the simulated solar exposure. The other study was conducted to
30 gain insight into the changes in the distribution of oil photoproducts caused by photo-
31 oxygenation.⁵⁹ Excitation-emission matrix spectroscopy was utilized to examine oil, interfacial
32 material (IM), and dissolved organic matter (DOM). The DOM was gathered and concentrated
33 using solid-phase extraction, and the extracts, as well as the oil and IM samples, were subjected
34 to analysis using negative-ion ESI in conjunction with FT-ICR MS.
35
36
37
38

39 Vaughan et al¹³⁰ studied how the water accommodated fractions (WAF) of MC252 and a
40 surrogate oil changed when exposed to photochemical effects. They used FT-ICR MS data to
41 make a molecular-level comparison between the two oils. The original substances of the two oils
42 were similar in terms of their elemental composition, except for the amount of oxygen present. In
43 MC252, the oxygen content was 0.4%, while in the surrogate oil, it was 5.36%. Additionally, the
44 results obtained through (-) ESI FT-ICR MS analysis indicated the prevalence of hydrocarbon
45 chains (HC) and the abundance of heteroatoms N₁, NO, and O₁ in both oils. The study also
46 revealed that both types of crude oil had similar average numbers of DBE and carbon atoms
47 within each elemental class. In the meantime, the distribution of classes of heteroatoms,
48 including HC, N₁, O₁, and S₁, was demonstrated by APPI in both oils. These heteroatom classes
49 showed similarities in distribution in both oils to some extent, except HC, S₁ and oxygenated
50 compounds with up to O₆, which were increased in surrogate compared to MC252 oil.
51 Additionally, the identification of the WSO fraction, which is acidic, was carried out using FT-
52 ICR MS, after one week incubation period for both oils. The results indicated the emergence of
53 N₁ and S₁O₃ species in surrogate oil samples that were kept in the dark, while a significant
54
55
56
57
58
59
60

amount of S_1O_4 was detected in samples that were subjected to photosynthetically active radiation (PAR) during incubation. Other heteroatom classes such as species containing N, N_1O_1 , or N_1O_2 were observed in the samples exposed to natural sunlight. Regarding the MC252 samples, certain variations were observed in their behavior as compared to the surrogate oil. In the dark samples of the MC252, there were no alterations detected in the heteroatom species except for the creation of S_1O_3 . While samples exposed to PAR exhibited a decrease in O_2 over the course of 6 exposure days, they also experienced a significant increase in O_4 - O_6 and N_1O_{3-5} species. The full sun irradiated samples, on the other hand, experienced formation of N_1O_4 , S_1O_4 , and N_1O_5 containing species. The authors hypothesized that the behavior of the S_1O_x and N_1 species was responsible for these variations in the formation of these heteroatom species. The (-) FT-ICR MS analysis of the acidic species heteroatom distribution revealed variations between the two oil samples. In contrast to the irradiated surrogate oil, which generated N_1O_1 and N_1O_2 at lower concentrations, the irradiated MC252 produced N_1O_x at higher concentrations together with S_1O_3 and S_1O_4 production. Moreover, after day one of irradiation, surrogate oil produced oxygenated species (O_{3-5} classes) at a faster rate than MC252 oil, and the results showed in general that the surrogate oil was oxidized over a wider range of carbon numbers than MC252.

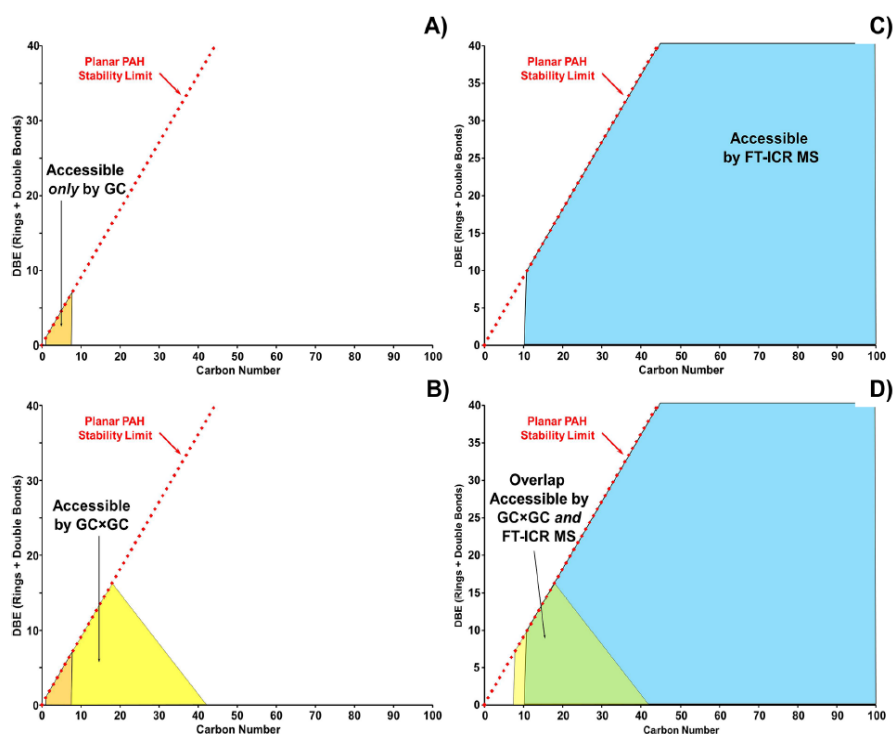


Fig. 8. Schematic diagram of the compositional continuum of petroleum (the petroleome) reported as double bond equivalents (DBE, number of rings plus double bonds) versus carbon number. The analytical window accessible only by conventional gas chromatography (GC) is displayed in part a, with the upper boundary limit for all molecules known to exist in petroleum displayed as the PAH planar stability limit, as previously reported (see text). Extension to hybrid analytical techniques (GC \times GC) is displayed in Fig 2b. Part c reports the extension to complete compositional coverage of petroleum molecules (up to C100) that have been observed in Macondo petroleum. Part d combines all three techniques in a single image to highlight the need for advanced analytical techniques beyond gas chromatography for oil spill science. Adapted from McKenna et al.¹²¹

Niles et al.,⁵⁶ studied the production of aldehydes and ketones in weathered oil using strong anion exchange solid-phase extraction. Then, employing a charged tag that specifically changes ketone/aldehyde-containing molecules, ketones and aldehydes were derivatized and enriched. The charged tag ampliflex keto reagent was mixed with the ketone/aldehyde fractions for

1
2
3 derivatization, and high-resolution FT-ICR MS analysis was then performed. Islam et al,⁴ in their
4 work on the spilled oil from the Hebei Spirit applied atmospheric pressure photo-ionization
5 hydrogen/deuterium exchange mass spectrometry to determine the compositional changes after
6 weathering of oil. The resin fractions were obtained from applying the SARA technique.^{14,131}
7

8 Employing ultrahigh-resolution FT-ICR MS in the analysis of oil spills showed effective
9 analytical capabilities, allowing for a more comprehensive understanding of the composition and
10 fate of spilled oil. Moreover, the capability to detect less polar compounds, which are
11 inaccessible by GC, enhances the ability to track the transformation and degradation of spilled
12 oil over time, providing development of effective remediation strategies. Additionally, the
13 molecular-level compositional characterization of the oil samples from DWH oil spill provides
14 analytical data which can serve as a baseline for comparison with subsequent samples collected
15 from other spill locations. Furthermore, the FT-ICR MS showed efficiency when combined with
16 different ionization techniques such as ESI, APPI and PSI for identification of thousands of
17 elemental compositions of heteroatom-containing species in oil samples. Moreover, the use of
18 PCA of elemental composition data obtained by FT-ICR MS can accurately identify the source of
19 environmental contamination caused by oil spills. However, there are still potential limitations of
20 using PCA for oil spill source identification. Through the reviewed articles, the FT-ICR MS
21 analysis showed a noticeable effectiveness for detecting the molecular changes in oil, however
22 exploring the integration of other analytical techniques that could provide complementary
23 information needs more effort.
24
25
26

27 *GC hybrid with other analysis techniques*

28
29 The 1950's launched the start of GC in petroleum analysis, which introduced for the first time an
30 approach for characterization of light petroleum gases of low boiling points such as methane,
31 ethane, and propane at a molecular level.¹³² However, it is generally restricted to compounds
32 boiling below 400 °C, resulting in the need for hybridization approaches. King et al,⁵⁸ studied the
33 photodegradation of oil samples collected after the DWH oil spill to explore the oil
34 photodegradation process under influencing environmental conditions. The authors applied GC-
35 FID in analysis of the oil samples after extraction of alkanes by dichloromethane and
36 fluorescence for PAHs. Distinguishable photodegradation activity was recorded especially for
37 high molecular weight PAHs.
38
39

40 Zito and Tarr⁴⁸ used GC to track the cis-trans photoisomerization transformation of 1,3-
41 pentadiene in spilled oil on GoM water as a function of irradiation time for the photochemical
42 production of organic triplets. The energies of the triplet states in the irradiated oil were found to
43 be in the 280–300 kJ/mol range. In a detailed analytical study, Aeppli et al,¹⁷ monitored the
44 compositional changes and determined the weathering processes that contributed to changes in
45 MW oil throughout 18 months after the spill. Saturate fraction (F_{Sat}), aromatic fraction (F_{Aro}),
46 and oxygenated fractions (F_{Oxy1} , and F_{Oxy2}) were extracted by a silica-gel flash column technique
47 from 146 samples collected from impacted rock scrapings, sea surface, sand patties, and oil
48 slicks. The saturated, aromatic, and oxygenated fraction content were estimated using TLC-FID
49 and GC-FID. GC-MS as previously published.^{14,121} Moreover, the biomarker ratios in this study
50 were detected with comprehensive two-dimensional GC (GC×GC) using GC×GC-FID and
51 GC×GC-MS techniques.¹³³
52
53

54
55 A study of the contribution of photooxidized PASHs to toxicity of water from Egyptian crude oil
56 samples was done by Fathalla and Andersson.⁶⁵ Column chromatography was used for
57
58
59
60

1
2
3 fractionation of oil samples into saturates and aromatics using *n*-heptane and toluene as elution
4 solvents for the PASHs. A medium pressure mercury lamp (TQ150, 250 W, Heraeus) was
5 applied for simulated photooxidation of PASHs, and the photooxidized products were extracted
6 with dichloroethane. *N,O*-bis(trimethylsilyl)trifluoroacetamide was used for derivatization of
7 the isolated photooxidized species. GC-MS and (-) ESI TOF-MS were applied to achieve a deep
8 understanding of elemental composition and changes.
9

10 Lemkau et al,¹³⁴ conducted a detailed qualitative and quantitative compositional characterization
11 of transformed heavy oil products following the oil spilled from Cosco Busan HFO (San
12 Francisco, CA, 2007) over 80 days by GC and GCxGC. The weathering at different sites varied,
13 but in general, the compounds which has a shorter GC retention time than *n*-C16 were depleted
14 due to evaporation and dissolution. Changes in the ratios of *n*-C18 to phytane and
15 benz[a]anthracene to chrysene indicated that biodegradation and photodegradation took place.
16 MS combined with PSI was applied by Kim et al,¹⁰⁵ to study the molecular level
17 characterization of compounds of the spilled oil. PSI is an effective analysis tool for polar
18 compounds.^{135,136} This study used sodium dodecyl sulfate because it had an excellent response in
19 negative PSI-MS. With PSI-MS, the quantitative analysis can be conducted with as little as 2
20 µg of sample amount. PSI-MS was also used to successfully evaluate oil solutions contaminated
21 with up to 0.05 % NaCl. In addition, the influence of NaCl contamination on the MS signal was
22 considered while evaluating the PSI potential.
23
24
25

26 Since aldehyde and ketone photoproducts are dissolvable in the aqueous phase in the irradiated
27 oil-water system after photoproduction, the Tarr group developed an effective approach for
28 better understanding their production. This work used MS/MS to identify the fragmentation of
29 aldehyde and ketone DNPH derivatives after derivatization with 2,4-dinitrophenylhydrazine
30 (DNPH).⁵⁵ Most of the detected aldehydes and ketones were multifunctional compounds,
31 whereas the single aldehydes or ketones were rare.
32
33

34 By combining several different analytical methods, including two-dimensional gas
35 chromatography and mass spectrometry (GCxGC-MS), flame ionization detection (GCxGC-
36 FID), and electrospray ionization (ESI) with FT-ICR MS, Chen et al.⁹⁶ were able to determine
37 how Macondo well oil extracted from Louisiana salt marsh sediments underwent molecular
38 transformation. In another study done by the Aepli group,⁹¹ monitoring the oxygenated,
39 weathering products of DWH oil and detecting their precursors was achieved by analysis of 41
40 oil samples, including surface slicks collected directly after the DWH spill in 2010 from May to
41 June, and rocks covered with oil and debris collected in 2011 from July to November. In this
42 study, GCxGC-FID hybrid with and GCxGC-(TOF-MS) was applied. A partial least squares
43 model was applied to match the resulting chromatograms from previous techniques with the
44 TLC-FID measured saturate, aromatic, and oxygenated factions to detect the precursors of the
45 oxygenated weathered products.
46
47

48 The use of GC analysis, such as GC-FID and GCxGC, contributes to the quantification of oil weathering
49 photoproducts. The findings emphasize the importance of expanding analytical methods, including GC-
50 based analysis, to gain a comprehensive understanding of the fate and transformation of oil. The use of
51 comprehensive GCxGC and chemometric techniques allowed for the analysis of a large number of
52 samples. While this method offers valuable insights into the chemodynamic processes involved in the oil
53 spill, it's important to note that it has limitations in terms of the accuracy and precision of the analysis.
54 Moreover, a deeper understanding of the weathering processes and fate of spilled oil could be achieved in
55
56
57

1
2
3 future studies which incorporate comprehensive GC×GC as part of their analytical approach. This
4 technique allows for a more detailed analysis of the unresolved complex mixture of saturated
5 hydrocarbons, which are often buried in a single dimension GC chromatogram. These GC techniques are
6 limited due to the lower volatility of oxygenated products. Electrospray mass spectrometry provides
7 advantages for these materials, but some photoproducts are likely still undetected by methods used to
8 date. For example, polymerization type photoproducts are believed to occur but have not been observed.
9

10 *Fingerprinting of spilled oil*

11
12 Contribution of the analytical techniques in oil fingerprint identification of the spilled oil source
13 is a pivotal issue in studying the oil fate and gauging environmental threats to the ecosystem.
14 Tracking different recalcitrant compounds, which act as biomarkers for the oil source, relies
15 mainly on the combination of effective separation techniques and mass spectrometry. Lobodin et
16 al,¹³⁷ established the combination of GC with APCI MS/MS for the analysis of steranes,
17 diasteranes, and pentacyclic triterpenes biomarkers for Macondo well oil. In this study, the
18 authors employed seven diagnostic ratios that are frequently utilized to identify, correlate, and
19 distinguish spilled oils.¹³⁸ All examined samples discovered between one month and almost four
20 years after the accident showed a substantial resemblance to NIST 2779, illustrating the stability
21 of the biomarker ratios over an extended period of time.
22
23

24 In another forensic study done by Aepli et al,¹³⁹ 50 oiled samples from the DWH oil spill were
25 used to investigate the contribution of solar irradiation intensity and higher temperature in
26 degradation of the biomarkers of Macondo well oil. GC-MS data for 28 samples were used for
27 measuring biomarker concentrations. Thin-layer chromatography combined with flame
28 ionization detection (TLC-FID) was applied to determine the concentration of oxygenated
29 hydrocarbons. The samples of oily sand lost volatile compounds with less than 15 carbons, and
30 dissolution of compounds with high polarity was observed.¹⁴⁰ While, there was a depletion in
31 other fractions such as alkanes, there were some biomarkers such as diasteranes and hepanoids,
32 which had enrichment in their concentrations during weathering. In comparison to triaromatic
33 steranes (TAS), the authors discovered that lower-molecular-weight TAS were lost more
34 frequently. Consequently, they ruled out biodegradation as the main mechanism of TAS
35 degradation. The photosensitivity of TAS results from their aromatic backbones.¹²⁵ Additionally,
36 abiotic oxidation processes have been associated with TAS depletion in weathered bitumens and
37 crude oil seeps.
38
39
40

41 APPI FT-ICR MS was used for identification of chemical changes in samples from the 2007
42 M/V Cosco Busan heavy fuel oils (HFO) spill by Lemkau et al.¹⁴¹ A bulk elemental analysis
43 revealed alterations in the total weight percentages of sulfur, oxygen, nitrogen, carbon, and
44 hydrogen on a global scale. The findings indicated that there were no noteworthy variations in
45 the nitrogen content between the parent sample with a weight percentage of 0.53% and the
46 weathered oil samples with a content of 1.0% after 617 days. Similarly, the sulfur levels found in
47 the samples collected from the field (ranging from 1.5% to 1.9%) were not significantly different
48 from the original value of sulfur found in the parent HFO (which was 1.8%). The drastic change
49 was in the oxygen content, which increased by three times compared to the parent compounds
50 (1.8% by weight) to about 6.6% by weight in the post-spill samples. This increase was attributed
51 to the production of oxygenated species. The percent mass of the oxygenated fraction of the
52 parent HFO was 31%, which increased by more than double in the samples collected after 296
53 days (64%) and reached 78% after 617 days. From the data obtained from FT-ICR MS, the
54
55
56
57
58
59
60

1
2
3 distribution of molecular weights in the parent HFO extended to 650 m/z and declined to 325
4 m/z after 617 days of weathering. The increase in the abundance of compounds containing two
5 oxygen atoms was attributed to the oxidation of compounds with one oxygen atom (such as
6 alcohols, aldehydes, and ketones) to acids.¹⁴² The compositional changes obtained by FT-ICR
7 MS showed a similar trend of different heteroatom classes in terms of carbon atom numbers and
8 DBE distribution.
9

10 Radović et al,⁶² examined the role of photochemical processes in analysis of the fingerprints of
11 the oil spill. The sample extracts were sequentially eluted on silica-coated quartz rods using
12 solvents of increasing polarity (*n*-hexane, *n*-hexane:toluene, and methanol:DCM), resulting in
13 four different classes: saturates (S), aromatics (Ar), and two polar fractions (PI),. They used
14 Fourier transform infrared spectroscopy (FT-IR) and (PII) besides GC-MS and GCxGC-FID.
15 For both heavy (Prestige) and light (Macondo) crude oils tested in this work, there was a
16 depletion in aromatic and saturate fractions and a significant increase in polar compounds. It was
17 noticed that the level of photooxidation in the aromatic hydrocarbons increased significantly as
18 the degree of alkylation in the aromatic backbone increased. This increase in photoactivity was
19 also aligned with the increase in the number of aromatic rings in the molecule. The authors
20 attributed this behavior to the enrichment of the electronic density of the π system for extended
21 conjugation. For instance, chrysene molecules showed more depletion than phenanthrenes.
22 Furthermore, there was a notable contrast in photoactivity observed between peri-condensed
23 structures such as pyrene and cata-condensed structures such as fluoranthene. Sulfur-containing
24 compounds showed an unexpected decrease in photodegradation. The S atom should be a
25 suitable site for oxidation, but its activity differs in aqueous solutions.¹⁰⁷ In contrast, the presence
26 of nitrogen containing heteroatom compounds (e.g., carbazole derivatives) enhanced the
27 photooxidation. The authors introduced data about recalcitrant properties of other triaromatic
28 sterane biomarkers. While those biomarkers are considered to be recalcitrant and were used in oil
29 fingerprinting after the Exxon Valdez spill, the irradiated samples in this study showed a
30 decrease in the amounts of these compounds by nearly 20%. Another significant decrease in the
31 amount of TAS by 87.5% was shown for rock scraping samples containing Macondo well oil
32 from the GoM. The influence of photooxidation on TAS biomarkers stability was also assessed
33 under lab conditions. The amount of TAS depleted began within the first 24 hours of irradiation
34 and continued during the first week, until no TAS compounds were discovered at the end of the
35 trial (70 days). The authors also ascribed the loss of TAS in samples of rock scraping of
36 weathered Macondo oil from the GoM to the photooxidation rate with 11% loss per day during
37 the first irradiation week, highlighting the importance of the photooxidation process.
38 Consequently, photooxidation represents an important pathway for TAS decomposition that was
39 not previously considered. In addition to providing an understanding of phototransformation
40 processes, this study demonstrates that accepted oil fingerprinting methods are subject to errors
41 when photochemical weathering is involved.
42
43
44
45
46
47

48 Arekhi et al¹⁴³ employed the highly recalcitrant C30 $\alpha\beta$ -hopane as an internal biomarker to gauge
49 the degradation degrees of various biomarker compounds and make assessments about the
50 overall extent of weathering in the oil spill residues. The authors also assessed the stability of the
51 relative diagnostic ratios of the biomarkers over a decade. Moreover, they compared the
52 degradation levels of different biomarker compounds and offered understanding into what
53 happens to these compounds over the long term within the oil spill residues. The results showed
54 that throughout the 10-year duration of the study, four tricyclic terpanes with lower molecular
55
56
57

1
2
3 weights, three steranes with lower molecular weights, and all triaromatic steranes exhibited
4 degradation. Meanwhile, other terpanes and steranes remained resistant to degradation. After a
5 decade of undergoing natural weathering, the homohopanes remained resistant to degradation.
6 Although there was some degradation, the diagnostic ratios of the biomarkers within all the three
7 groups remained consistent over the 10-year timeframe. Moreover, the study offered significant
8 understanding of the long-term fate and degradation of petroleum biomarkers in DWH oil spill
9 residues. Identifying particular biomarker compounds that persist unchanged after 10 years of
10 natural weathering can provide valuable insights for crafting improved oil spill remediation
11 strategies. The study did not explore the potential interactions or transformations of the
12 biomarker compounds with various environmental factors or components, which could have an
13 impact on their degradation patterns and ultimate fate.
14
15

16
17 The reviewed articles conducted correlation analyses to evaluate the resemblance between environmental
18 samples and the oil spill, providing valuable data for differentiation of potential sources. Combining
19 results from high resolution FT-ICR MS with GC-based data provides a more comprehensive
20 understanding of oil spill weathering. Overall, the studies demonstrated the effects of photooxidation on
21 the composition of spilled oils caused by natural and simulated sunlight. However, there is still a need to
22 extend the range of molecular markers and ratios to achieve reliable differentiation between closely
23 related sources and provide statistical parameters for fingerprinting the oil spill. Further research is
24 required to consider the overall ecological, geographical and climatic factors that could influence the
25 effectiveness of fingerprinting methods under different conditions. It would be valuable to conduct
26 comparative studies on different oil spill scenarios to assess the generalizability of the observed molecular
27 transformations and to identify any unique characteristics of specific oil types. Despite some advances,
28 the full impact of photochemistry on biomarker persistence and reliability is still uncertain.
29
30

31 **Conclusion**

32
33 The DWH oil spill was a devastating event that resulted in massive amounts of oil being released
34 into aquatic systems. Since then, there have been significant developments in understanding the
35 photochemistry of oil in these systems. Researchers have made great strides in identifying the
36 different pathways of oil photodegradation, as well as the factors that influence its photochemical
37 fate. These developments have important implications for the management and remediation of
38 oil spills in marine systems. They provided valuable information on the potential impacts of
39 sunlight on oil degradation, and the effectiveness of different remediation strategies. As we
40 continue to face the challenges of managing oil spills in oceans, ongoing studies of
41 photochemistry of oil in marine systems will be crucial for developing effective solutions that
42 can minimize the damage by these spills. Despite all of these efforts achieved in studying oil
43 photooxidation process on many levels such as the photoproducts and the influential
44 environmental factors, there are still many challenges in completely explaining the
45 photooxidation process. Moreover, comparing environmental studies to lab studies is infrequent,
46 and not enough work has established connections between molecular level observations and
47 environmental behavior. Specific areas that need additional study are the prediction of
48 photoproduct distributions and properties under varied environmental conditions (solar intensity
49 and duration, temperature, NOM, etc.); understanding photoproduct impact on emulsification;
50 characterizing the interplay between photochemistry, biodegradation, and toxicity; and toxicity
51 impacts across organisms. It is obvious from the findings of the prior studies under review that
52 the detailed photochemical steps in solar driven weathering need further study to be understood.
53
54
55
56
57
58
59
60

Acknowledgements:

This project was partially supported by the U.S. National Science Foundation (NSF-2038312).

Author contributions:

M.E. gathered references and wrote the bulk of the initial manuscript. L.M. gathered references and wrote the material on biological systems. M.A.T. oversaw the project and revised the manuscript to its final form.

Acknowledgments

This project was partially supported by the U.S. National Science Foundation (NSF-2038312).

References

- (1) Routoula, E.; Patwardhan, S. V. Degradation of Anthraquinone Dyes from Effluents: A Review Focusing on Enzymatic Dye Degradation with Industrial Potential. *Environ. Sci. Technol.* **2020**, *54* (2), 647–664. <https://doi.org/10.1021/acs.est.9b03737>.
- (2) O'Reilly, C.; Silva, M.; Daneshgar Asl, S.; Meurer, W. P.; MacDonald, I. R. Distribution, Magnitude, and Variability of Natural Oil Seeps in the Gulf of Mexico. *Remote Sensing* **2022**, *14* (13), 3150. <https://doi.org/10.3390/rs14133150>.
- (3) Kvenvolden, K. A.; Cooper, C. K. Natural Seepage of Crude Oil into the Marine Environment. *Geo-Mar Lett* **2003**, *23* (3), 140–146. <https://doi.org/10.1007/s00367-003-0135-0>.
- (4) Islam, A.; Kim, D.; Yim, U. H.; Shim, W. J.; Kim, S. Structure-Dependent Degradation of Polar Compounds in Weathered Oils Observed by Atmospheric Pressure Photo-Ionization Hydrogen/Deuterium Exchange Ultrahigh Resolution Mass Spectrometry. *Journal of Hazardous Materials* **2015**, *296*, 93–100. <https://doi.org/10.1016/j.jhazmat.2015.04.042>.
- (5) Li, K.; Yu, H.; Yan, J.; Liao, J. Analysis of Offshore Oil Spill Pollution Treatment Technology. *IOP Conf. Ser.: Earth Environ. Sci.* **2020**, *510* (4), 042011. <https://doi.org/10.1088/1755-1315/510/4/042011>.
- (6) Li, P.; Cai, Q.; Lin, W.; Chen, B.; Zhang, B. Offshore Oil Spill Response Practices and Emerging Challenges. *Marine Pollution Bulletin* **2016**, *110* (1), 6–27. <https://doi.org/10.1016/j.marpolbul.2016.06.020>.
- (7) Liu, S.; Wang, Y.; Liang, Y. Environmental Consequence Analysis of Oil Spills from Onshore Pipelines with Parametric Uncertainty. *Process Safety and Environmental Protection* **2020**, *141*, 123–134. <https://doi.org/10.1016/j.psep.2020.04.032>.
- (8) Kheraj, S. A History of Oil Spills on Long-Distance Pipelines in Canada. *Canadian Historical Review* **2020**, *101* (2), 161–191. <https://doi.org/10.3138/chr.2019-0005>.
- (9) Aroh, K. N.; Ubong, I. U.; Eze, C. L.; Harry, I. M.; Umo-Otong, J. C.; Gobo, A. E. Oil Spill Incidents and Pipeline Vandalization in Nigeria. *Disaster Prevention and Management: An International Journal* **2010**, *19* (1), 70–87. <https://doi.org/10.1108/09653561011022153>.
- (10) Ivshina, I. B.; Kuyukina, M. S.; Krivoruchko, A. V.; Elkin, A. A.; Makarov, S. O.; Cunningham, C. J.; Peshkur, T. A.; Atlas, R. M.; Philp, J. C. Oil Spill Problems and

- Sustainable Response Strategies through New Technologies. *Environ. Sci.: Processes Impacts* **2015**, *17* (7), 1201–1219. <https://doi.org/10.1039/C5EM00070J>.
- (11) Major, D. N.; Wang, H. How Public Health Impact Is Addressed: A Retrospective View on Three Different Oil Spills. *Toxicological & Environmental Chemistry* **2012**, *94* (3), 442–467. <https://doi.org/10.1080/02772248.2012.654633>.
- (12) Kessler, J. D.; Valentine, D. L.; Redmond, M. C.; Du, M.; Chan, E. W.; Mendes, S. D.; Quiroz, E. W.; Villanueva, C. J.; Shusta, S. S.; Werra, L. M.; Yvon-Lewis, S. A.; Weber, T. C. A Persistent Oxygen Anomaly Reveals the Fate of Spilled Methane in the Deep Gulf of Mexico. *Science* **2011**, *331* (6015), 312–315.
- (13) Camilli, R.; Reddy, C. M.; Yoerger, D. R.; Van Mooy, B. A. S.; Jakuba, M. V.; Kinsey, J. C.; McIntyre, C. P.; Sylva, S. P.; Maloney, J. V. Tracking Hydrocarbon Plume Transport and Biodegradation at Deepwater Horizon. *Science* **2010**, *330* (6001), 201–204.
- (14) Reddy, C. M.; Arey, J. S.; Seewald, J. S.; Sylva, S. P.; Lemkau, K. L.; Nelson, R. K.; Carmichael, C. A.; McIntyre, C. P.; Fenwick, J.; Ventura, G. T.; Van Mooy, B. A. S.; Camilli, R. Composition and Fate of Gas and Oil Released to the Water Column during the Deepwater Horizon Oil Spill. *Proceedings of the National Academy of Sciences* **2012**, *109* (50), 20229–20234. <https://doi.org/10.1073/pnas.1101242108>.
- (15) Valentine, D. L.; Kessler, J. D.; Redmond, M. C.; Mendes, S. D.; Heintz, M. B.; Farwell, C.; Hu, L.; Kinnaman, F. S.; Yvon-Lewis, S.; Du, M.; Chan, E. W.; Tigreros, F. G.; Villanueva, C. J. Propane Respiration Jump-Starts Microbial Response to a Deep Oil Spill. *Science* **2010**, *330* (6001), 208–211.
- (16) Hazen, T. C.; Dubinsky, E. A.; DeSantis, T. Z.; Andersen, G. L.; Piceno, Y. M.; Singh, N.; Jansson, J. K.; Probst, A.; Borglin, S. E.; Fortney, J. L.; Stringfellow, W. T.; Bill, M.; Conrad, M. E.; Tom, L. M.; Chavarria, K. L.; Alusi, T. R.; Lamendella, R.; Joyner, D. C.; Spier, C.; Baelum, J.; Auer, M.; Zemla, M. L.; Chakraborty, R.; Sonnenthal, E. L.; D'haeseleer, P.; Holman, H.-Y. N.; Osman, S.; Lu, Z.; Van Nostrand, J. D.; Deng, Y.; Zhou, J.; Mason, O. U. Deep-Sea Oil Plume Enriches Indigenous Oil-Degrading Bacteria. *Science* **2010**, *330* (6001), 204–208.
- (17) Aeppli, C.; Carmichael, C. A.; Nelson, R. K.; Lemkau, K. L.; Graham, W. M.; Redmond, M. C.; Valentine, D. L.; Reddy, C. M. Oil Weathering after the *Deepwater Horizon* Disaster Led to the Formation of Oxygenated Residues. *Environ. Sci. Technol.* **2012**, *46* (16), 8799–8807. <https://doi.org/10.1021/es3015138>.
- (18) Lozano, D. C. P.; Gavard, R.; P. Arenas-Diaz, J.; J. Thomas, M.; D. Stranz, D.; Mejía-Ospino, E.; Guzman, A.; F. Spencer, S. E.; Rossell, D.; P. Barrow, M. Pushing the Analytical Limits: New Insights into Complex Mixtures Using Mass Spectra Segments of Constant Ultrahigh Resolving Power. *Chemical Science* **2019**, *10* (29), 6966–6978. <https://doi.org/10.1039/C9SC02903F>.
- (19) Overton, E. B.; Wade, T. L.; Radović, J. R.; Meyer, B. M.; Miles, M. S.; Larter, S. R. Chemical Composition of Macondo and Other Crude Oils and Compositional Alterations During Oil Spills. *Oceanography* **2016**, *29* (3), 50–63.
- (20) Cheong, S.-M. Fishing and Tourism Impacts in the Aftermath of the Hebei-Spirit Oil Spill. *Journal of Coastal Research* **2012**, *28* (6), 1648–1653. <https://doi.org/10.2112/JCOASTRES-D-11-00079.1>.
- (21) Overton, E. B.; Wade, T. L.; Radović, J. R.; Meyer, B. M.; Miles, M. S.; Larter, S. R. Chemical Composition of Macondo and Other Crude Oils and Compositional Alterations During Oil Spills. *Oceanography* **2016**, *29* (3), 50–63.

- 1
2
3 (22) Gohlke, J. M.; Doke, D.; Tipre, M.; Leader, M.; Fitzgerald, T. A Review of Seafood
4 Safety after the Deepwater Horizon Blowout. *Environmental Health Perspectives* **2011**, *119*
5 (8), 1062–1069. <https://doi.org/10.1289/ehp.1103507>.
6
7 (23) Martin, C. W.; McDonald, A. M.; Valentine, J. F.; Roberts, B. J. Towards Relevant
8 Ecological Experiments and Assessments of Coastal Oil Spill Effects: Insights from the 2010
9 Deepwater Horizon Oil Spill. *Frontiers in Environmental Science* **2023**, *10*.
10 (24) Montagna, P. A.; Arismendez, S. S. Crude Oil Pollution II. Effects of the Deepwater
11 Horizon Contamination on Sediment Toxicity in the Gulf of Mexico. *A handbook of*
12 *environmental toxicology: human disorders and ecotoxicology* **2020**, 311–319.
13 <https://doi.org/10.1079/9781786394675.0311>.
14 (25) *Validation of oil fate and mass balance for the Deepwater Horizon oil spill: Evaluation*
15 *of water column partitioning - ScienceDirect*.
16 <https://www.sciencedirect.com/science/article/pii/S0025326X21010985> (accessed 2023-08-
17 29).
18 (26) Radović, J. R.; Oldenburg, T. B. P.; Larter, S. R. Chapter 19 - Environmental Assessment
19 of Spills Related to Oil Exploitation in Canada's Oil Sands Region. In *Oil Spill*
20 *Environmental Forensics Case Studies*; Stout, S. A., Wang, Z., Eds.; Butterworth-
21 Heinemann, 2018; pp 401–417. <https://doi.org/10.1016/B978-0-12-804434-6.00019-7>.
22 (27) Omar, M. Y.; Shehada, M. F.; Mehanna, A. K.; Elbatran, A. H.; Elmesiry, M. M. A Case
23 Study of the Suez Gulf: Modelling of the Oil Spill Behavior in the Marine Environment. *The*
24 *Egyptian Journal of Aquatic Research* **2021**, *47* (4), 345–356.
25 <https://doi.org/10.1016/j.ejar.2021.10.005>.
26 (28) Govindarajan, S. K.; Mishra, A.; Kumar, A. Oil Spill in a Marine Environment:
27 Requirements Following an Offshore Oil Spill. *Rudarsko-geološko-naftni zbornik* **2021**, *36*
28 (4). <https://doi.org/10.17794/rgn.2021.4.1>.
29 (29) Soussi, A.; Bersani, C.; Sacile, R.; Bouchta, D.; Amarti, A. E.; Seghioer, H.; Nachite,
30 D.; Miys, J. A. An Oil Spill Trajectory Model: Validation in the Mediterranean Sea. In *2019*
31 *International Symposium on Systems Engineering (ISSE)*; 2019; pp 1–6.
32 <https://doi.org/10.1109/ISSE46696.2019.8984542>.
33 (30) Liu, H.; Sun, B.; Guan, L.; Yan, Z. Y. Dissolution and Photodegradation of Two Crude
34 Oils in Seawater. *Advanced Materials Research* **2013**, *726–731*, 556–559.
35 <https://doi.org/10.4028/www.scientific.net/AMR.726-731.556>.
36 (31) Chakravarthy, A.-R. Fates of Spilt Oil and Factors Affecting the Bio-Degradation of Oil:
37 A Review. *Theses* **2015**.
38 (32) Monteiro, C. B.; Oleinik, P. H.; Lopes, B. V.; Leal, T. F.; Junior, O. O. M.; Marques, W.
39 C. Oil Spill Simulations and Susceptibility in Coastal and Estuarine Areas. *Defect and*
40 *Diffusion Forum* **2019**, *396*, 109–120.
41 <https://doi.org/10.4028/www.scientific.net/DDF.396.109>.
42 (33) Harriman, B. H.; Zito, P.; Podgorski, D. C.; Tarr, M. A.; Suflita, J. M. Impact of
43 Photooxidation and Biodegradation on the Fate of Oil Spilled During the Deepwater Horizon
44 Incident: Advanced Stages of Weathering. *Environ. Sci. Technol.* **2017**, *51* (13), 7412–7421.
45 <https://doi.org/10.1021/acs.est.7b01278>.
46 (34) *Persistence and photochemical transformation of water soluble constituents from*
47 *industrial crude oil and natural seep oil in seawater - ScienceDirect*.
48 <https://www.sciencedirect.com/science/article/pii/S0025326X21000837> (accessed 2023-08-
49 29).
50
51
52
53
54
55
56
57
58
59
60

- 1
2
3
4
5
6
7
8
9
10
11
12
13
14
15
16
17
18
19
20
21
22
23
24
25
26
27
28
29
30
31
32
33
34
35
36
37
38
39
40
41
42
43
44
45
46
47
48
49
50
51
52
53
54
55
56
57
58
59
60
- (35) Schreiber, L.; Hunnie, B.; Altshuler, I.; Góngora, E.; Ellis, M.; Maynard, C.; Tremblay, J.; Wasserscheid, J.; Fortin, N.; Lee, K.; Stern, G.; Greer, C. W. Long-Term Biodegradation of Crude Oil in High-Arctic Backshore Sediments: The Baffin Island Oil Spill (BIOS) after Nearly Four Decades. *Environmental Research* **2023**, *233*, 116421. <https://doi.org/10.1016/j.envres.2023.116421>.
- (36) Prartono, T.; Dwinovantyo, A.; Syafrizal, S.; Syakti, A. D. Potential Use of Deep-Sea Sediment Bacteria for Oil Spill Biodegradation: A Laboratory Simulation. *Microorganisms* **2022**, *10* (8), 1616. <https://doi.org/10.3390/microorganisms10081616>.
- (37) Wang, C.; Liu, X.; Guo, J.; Lv, Y.; Li, Y. Biodegradation of Marine Oil Spill Residues Using Aboriginal Bacterial Consortium Based on Penglai 19-3 Oil Spill Accident, China. *Ecotoxicology and Environmental Safety* **2018**, *159*, 20–27. <https://doi.org/10.1016/j.ecoenv.2018.04.059>.
- (38) *Sunlight-driven dissolution is a major fate of oil at sea | Science Advances*. <https://www.science.org/doi/full/10.1126/sciadv.abl7605> (accessed 2023-09-21).
- (39) Council, N. R.; Sciences, D. on E. and P.; Applications, C. on P. S., Mathematics, and; Update, S. C. for the P. in the M. E. *Oil in the Sea: Inputs, Fates, and Effects*; National Academies Press, 1985.
- (40) Ward, C. P.; Overton, E. B. How the 2010 Deepwater Horizon Spill Reshaped Our Understanding of Crude Oil Photochemical Weathering at Sea: A Past, Present, and Future Perspective. *Environ. Sci.: Processes Impacts* **2020**, *22* (5), 1125–1138. <https://doi.org/10.1039/D0EM00027B>.
- (41) Lee, R. F. Photo-Oxidation and Photo-Toxicity of Crude and Refined Oils. *Spill Science & Technology Bulletin* **2003**, *8* (2), 157–162. [https://doi.org/10.1016/S1353-2561\(03\)00015-X](https://doi.org/10.1016/S1353-2561(03)00015-X).
- (42) Nicodem, D. E.; Fernandes, M. C. Z.; Guedes, C. L. B.; Correa, R. J. Photochemical Processes and the Environmental Impact of Petroleum Spills. *Biogeochemistry* **1997**, *39* (2), 121–138.
- (43) Zhou, Z.; Guo, L.; Shiller, A. M.; Lohrenz, S. E.; Asper, V. L.; Osburn, C. L. Characterization of Oil Components from the Deepwater Horizon Oil Spill in the Gulf of Mexico Using Fluorescence EEM and PARAFAC Techniques. *Marine Chemistry* **2013**, *148*, 10–21. <https://doi.org/10.1016/j.marchem.2012.10.003>.
- (44) Kujawinski, E. B.; Kido Soule, M. C.; Valentine, D. L.; Boysen, A. K.; Longnecker, K.; Redmond, M. C. Fate of Dispersants Associated with the Deepwater Horizon Oil Spill. *Environ. Sci. Technol.* **2011**, *45* (4), 1298–1306. <https://doi.org/10.1021/es103838p>.
- (45) *Comprehensive Analysis of Oil Sands Processed Water by Direct-Infusion Fourier-Transform Ion Cyclotron Resonance Mass Spectrometry with and without Offline UHPLC Sample Prefractionation | Environmental Science & Technology*. <https://pubs.acs.org/doi/abs/10.1021/es400813s> (accessed 2023-08-28).
- (46) Griffiths, M. T.; Da Campo, R.; O'Connor, P. B.; Barrow, M. P. Throwing Light on Petroleum: Simulated Exposure of Crude Oil to Sunlight and Characterization Using Atmospheric Pressure Photoionization Fourier Transform Ion Cyclotron Resonance Mass Spectrometry. *Anal. Chem.* **2014**, *86* (1), 527–534. <https://doi.org/10.1021/ac4025335>.
- (47) Zito, P.; Podgorski, D. C.; Bartges, T.; Guillemette, F.; Roebuck, J. A.; Spencer, R. G. M.; Rodgers, R. P.; Tarr, M. A. Sunlight-Induced Molecular Progression of Oil into Oxidized Oil Soluble Species, Interfacial Material, and Dissolved Organic Matter. *Energy Fuels* **2020**, *34* (4), 4721–4726. <https://doi.org/10.1021/acs.energyfuels.9b04408>.

- 1
2
3 (48) Ray, P. Z.; Tarr, M. A. Formation of Organic Triplets from Solar Irradiation of
4 Petroleum. *Marine Chemistry* **2015**, *168*, 135–139.
5 <https://doi.org/10.1016/j.marchem.2014.09.018>.
- 6 (49) Ray, P. Z.; Tarr, M. A. Solar Production of Singlet Oxygen from Crude Oil Films on
7 Water. *Journal of Photochemistry and Photobiology A: Chemistry* **2014**, *286*, 22–28.
8 <https://doi.org/10.1016/j.jphotochem.2014.04.016>.
- 9 (50) Ray, P. Z.; Chen, H.; Podgorski, D. C.; McKenna, A. M.; Tarr, M. A. Sunlight Creates
10 Oxygenated Species in Water-Soluble Fractions of Deepwater Horizon Oil. *Journal of*
11 *Hazardous Materials* **2014**, *280*, 636–643. <https://doi.org/10.1016/j.jhazmat.2014.08.059>.
- 12 (51) Ray, P. Z.; Tarr, M. A. Petroleum Films Exposed to Sunlight Produce Hydroxyl Radical.
13 *Chemosphere* **2014**, *103*, 220–227. <https://doi.org/10.1016/j.chemosphere.2013.12.005>.
- 14 (52) Saeed, T.; Ali, L. N.; Al-Bloushi, A.; Al-Hashash, H.; Al-Bahloul, M.; Al-Khabbaz, A.;
15 Al-Khayat, A. Effect of Environmental Factors on Photodegradation of Polycyclic Aromatic
16 Hydrocarbons (PAHs) in the Water-Soluble Fraction of Kuwait Crude Oil in Seawater.
17 *Marine Environmental Research* **2011**, *72* (3), 143–150.
18 <https://doi.org/10.1016/j.marenvres.2011.07.004>.
- 19 (53) Cao, X.; Tarr, M. A. Aldehyde and Ketone Photoproducts from Solar-Irradiated Crude
20 Oil–Seawater Systems Determined by Electrospray Ionization–Tandem Mass Spectrometry.
21 *Environ. Sci. Technol.* **2017**, *51* (20), 11858–11866. <https://doi.org/10.1021/acs.est.7b01991>.
- 22 (54) Tarr, M.; Zito, P.; Overton, E.; Olson, G.; Adkikari, P.; Reddy, C. Weathering of Oil
23 Spilled in the Marine Environment. *Oceanog* **2016**, *29* (3), 126–135.
24 <https://doi.org/10.5670/oceanog.2016.77>.
- 25 (55) Cao, X.; Tarr, M. A. Aldehyde and Ketone Photoproducts from Solar-Irradiated Crude
26 Oil–Seawater Systems Determined by Electrospray Ionization–Tandem Mass Spectrometry.
27 *Environ. Sci. Technol.* **2017**, *51* (20), 11858–11866. <https://doi.org/10.1021/acs.est.7b01991>.
- 28 (56) Niles, S. F.; Chacón-Patiño, M. L.; Chen, H.; McKenna, A. M.; Blakney, G. T.; Rodgers,
29 R. P.; Marshall, A. G. Molecular-Level Characterization of Oil-Soluble Ketone/Aldehyde
30 Photo-Oxidation Products by Fourier Transform Ion Cyclotron Resonance Mass
31 Spectrometry Reveals Similarity Between Microcosm and Field Samples. *Environ. Sci.*
32 *Technol.* **2019**, *53* (12), 6887–6894. <https://doi.org/10.1021/acs.est.9b00908>.
- 33 (57) King, S. M.; Leaf, P. A.; Tarr, M. A. Photochemistry of Deepwater Horizon Oil. In *It's*
34 *All in the Water: Studies of Materials and Conditions in Fresh and Salt Water Bodies*;
35 Benvenuto, M. A., Roberts-Kirchhoff, E. S., Murray, M. N., Garshott, D. M., Eds.; ACS
36 Symposium Series; American Chemical Society: Washington, DC, 2011; Vol. 1086, pp 81–
37 95. <https://doi.org/10.1021/bk-2011-1086.ch006>.
- 38 (58) King, S. M.; Leaf, P. A.; Olson, A. C.; Ray, P. Z.; Tarr, M. A. Photolytic and
39 Photocatalytic Degradation of Surface Oil from the Deepwater Horizon Spill. *Chemosphere*
40 **2014**, *95*, 415–422. <https://doi.org/10.1016/j.chemosphere.2013.09.060>.
- 41 (59) Zito, P.; Podgorski, D. C.; Bartges, T.; Guillemette, F.; Roebuck, J. A.; Spencer, R. G.
42 M.; Rodgers, R. P.; Tarr, M. A. Sunlight-Induced Molecular Progression of Oil into
43 Oxidized Oil Soluble Species, Interfacial Material, and Dissolved Organic Matter. *Energy*
44 *Fuels* **2020**, *34* (4), 4721–4726. <https://doi.org/10.1021/acs.energyfuels.9b04408>.
- 45 (60) Ward, C. P.; Sharpless, C. M.; Valentine, D. L.; Aeppli, C.; Sutherland, K. M.; Wankel,
46 S. D.; Reddy, C. M. Oxygen Isotopes ($\delta^{18}\text{O}$) Trace Photochemical Hydrocarbon Oxidation
47 at the Sea Surface. *Geophys. Res. Lett.* **2019**, *46* (12), 6745–6754.
48 <https://doi.org/10.1029/2019GL082867>.
- 49
50
51
52
53
54
55
56
57
58
59
60

- 1
2
3 (61) Arekhi, M.; Terry, L. G.; Clement, T. P. Characterizing the Efficiency of Low-Cost LED
4 Lights for Conducting Laboratory Studies to Investigate Polycyclic Aromatic Hydrocarbon
5 Photodegradation Processes. *Environmental Research* **2023**, *217*, 114951.
6 <https://doi.org/10.1016/j.envres.2022.114951>.
- 7
8 (62) Radović, J. R.; Aeppli, C.; Nelson, R. K.; Jimenez, N.; Reddy, C. M.; Bayona, J. M.;
9 Albaigés, J. Assessment of Photochemical Processes in Marine Oil Spill Fingerprinting.
10 *Marine Pollution Bulletin* **2014**, *79* (1–2), 268–277.
11 <https://doi.org/10.1016/j.marpolbul.2013.11.029>.
- 12
13 (63) Saeed, T.; Ali, L.; Al-Bloushi, A.; Al-Hashash, H.; Bahloul, M.; Khabbaz, A.; Alkhatat,
14 A. Effect of Environmental Factors on Photodegradation of Polycyclic Aromatic
15 Hydrocarbons (PAHs) in the Water-Soluble Fraction of Kuwait Crude Oil in Seawater.
16 *Marine environmental research* **2011**, *72*, 143–150.
17 <https://doi.org/10.1016/j.marenvres.2011.07.004>.
- 18
19 (64) Liu, H.; Sun, B.; Guan, L.; Yan, Z. Y. Dissolution and Photodegradation of Two Crude
20 Oils in Seawater. *Advanced Materials Research* **2013**, *726–731*, 556–559.
21 <https://doi.org/10.4028/www.scientific.net/AMR.726-731.556>.
- 22
23 (65) Fathalla, E. M.; Andersson, J. T. Products of Polycyclic Aromatic Sulfur Heterocycles in
24 Oil Spill Photodegradation. *Environmental Toxicology and Chemistry* **2011**, *30* (9), 2004–
25 2012. <https://doi.org/10.1002/etc.607>.
- 26
27 (66) Kim, D.; Ha, S. Y.; An, J. G.; Cha, S.; Yim, U. H.; Kim, S. Estimating Degree of
28 Degradation of Spilled Oils Based on Relative Abundance of Aromatic Compounds
29 Observed by Paper Spray Ionization Mass Spectrometry. *Journal of Hazardous Materials*
30 **2018**, *359*, 421–428. <https://doi.org/10.1016/j.jhazmat.2018.07.060>.
- 31
32 (67) Zhang, Z. W.; Zhang, C. Photodegradation of Oily Waste Water Using Nano-TiO₂.
33 *Advanced Materials Research* **2011**, *332–334*, 2153–2156.
34 <https://doi.org/10.4028/www.scientific.net/AMR.332-334.2153>.
- 35
36 (68) Bacosa, H. P.; Erdner, D. L.; Liu, Z. Differentiating the Roles of Photooxidation and
37 Biodegradation in the Weathering of Light Louisiana Sweet Crude Oil in Surface Water
38 from the Deepwater Horizon Site. *Marine Pollution Bulletin* **2015**, *95* (1), 265–272.
39 <https://doi.org/10.1016/j.marpolbul.2015.04.005>.
- 40
41 (69) Shankar, R.; Shim, W. J.; An, J. G.; Yim, U. H. A Practical Review on Photooxidation of
42 Crude Oil: Laboratory Lamp Setup and Factors Affecting It. *Water Research* **2015**, *68*, 304–
43 315. <https://doi.org/10.1016/j.watres.2014.10.012>.
- 44
45 (70) *Hot and Cold: Photochemical Weathering Mediates Oil Properties and Fate Differently*
46 *Depending on Seawater Temperature | Environmental Science & Technology*.
47 <https://pubs.acs.org/doi/abs/10.1021/acs.est.3c02962> (accessed 2023-09-14).
- 48
49 (71) Wozniak, A. S.; Prem, P. M.; Obeid, W.; Waggoner, D. C.; Quigg, A.; Xu, C.; Santschi,
50 P. H.; Schwehr, K. A.; Hatcher, P. G. Rapid Degradation of Oil in Mesocosm Simulations of
51 Marine Oil Snow Events. *Environ. Sci. Technol.* **2019**, *53* (7), 3441–3450.
52 <https://doi.org/10.1021/acs.est.8b06532>.
- 53
54 (72) L. Harsha, M.; C. Redman, Z.; Wesolowski, J.; C. Podgorski, D.; L. Tomco, P.
55 Photochemical Formation of Water-Soluble oxyPAHs, Naphthenic Acids, and Other
56 Hydrocarbon Oxidation Products from Cook Inlet, Alaska Crude Oil and Diesel in Simulated
57 Seawater Spills. *Environmental Science: Advances* **2023**, *2* (3), 447–461.
58 <https://doi.org/10.1039/D2VA00325B>.

- 1
2
3 (73) Yin, F.; John, G. F.; Hayworth, J. S.; Clement, T. P. Long-Term Monitoring Data to
4 Describe the Fate of Polycyclic Aromatic Hydrocarbons in Deepwater Horizon Oil
5 Submerged off Alabama's Beaches. *Science of The Total Environment* **2015**, *508*, 46–56.
6 <https://doi.org/10.1016/j.scitotenv.2014.10.105>.
- 7
8 (74) *Weathering patterns of polycyclic aromatic hydrocarbons contained in submerged*
9 *Deepwater Horizon oil spill residues when re-exposed to sunlight - ScienceDirect.*
10 <https://www.sciencedirect.com/science/article/abs/pii/S0048969716317533> (accessed 2023-
11 09-21).
- 12 (75) Ray, P. Z.; Tarr, M. A.; Chen, H.; McKenna, A. M. Effect of Dispersant on Molecular
13 Composition and Fate of Oil Exposed to Sunlight in Seawater Systems. *International Oil*
14 *Spill Conference Proceedings* **2014**, *2014* (1), 300069. [https://doi.org/10.7901/2169-3358-
15 *2014-1-300069.1*.](https://doi.org/10.7901/2169-3358-2014-1-300069.1)
- 16 (76) Aeppli, C.; Mitchell, D. A.; Keyes, P.; Beirne, E. C.; McFarlin, K. M.; Roman-Hubers,
17 A. T.; Rusyn, I.; Prince, R. C.; Zhao, L.; Parkerton, T. F.; Nedwed, T. Oil Irradiation
18 Experiments Document Changes in Oil Properties, Molecular Composition, and Dispersant
19 Effectiveness Associated with Oil Photo-Oxidation. *Environ. Sci. Technol.* **2022**, *56* (12),
20 7789–7799. <https://doi.org/10.1021/acs.est.1c06149>.
- 21 (77) Zhao, X.; Liu, W.; Fu, J.; Cai, Z.; O'Reilly, S. E.; Zhao, D. Dispersion, Sorption and
22 Photodegradation of Petroleum Hydrocarbons in Dispersant-Seawater-Sediment Systems.
23 *Marine Pollution Bulletin* **2016**, *109* (1), 526–538.
24 <https://doi.org/10.1016/j.marpolbul.2016.04.064>.
- 25 (78) Gong, Y.; Fu, J.; O'Reilly, S. E.; Zhao, D. Effects of Oil Dispersants on
26 Photodegradation of Pyrene in Marine Water. *Journal of Hazardous Materials* **2015**, *287*,
27 142–150. <https://doi.org/10.1016/j.jhazmat.2015.01.027>.
- 28 (79) Ward, C. P.; Armstrong, C. J.; Conmy, R. N.; French-McCay, D. P.; Reddy, C. M.
29 Photochemical Oxidation of Oil Reduced the Effectiveness of Aerial Dispersants Applied in
30 Response to the *Deepwater Horizon* Spill. *Environ. Sci. Technol. Lett.* **2018**, *5* (5), 226–231.
31 <https://doi.org/10.1021/acs.estlett.8b00084>.
- 32 (80) Podgorski, D. C.; Walley, J.; Shields, M. P.; Hebert, D.; Harsha, M. L.; Spencer, R. G.
33 M.; Tarr, M. A.; Zito, P. Dispersant-Enhanced Photodissolution of Macondo Crude Oil: A
34 Molecular Perspective. *Journal of Hazardous Materials* **2024**, *461*, 132558.
35 <https://doi.org/10.1016/j.jhazmat.2023.132558>.
- 36 (81) Lee, J.; Hong, S.; Mackeyev, Y.; Lee, C.; Chung, E.; Wilson, L. J.; Kim, J.-H.; Alvarez,
37 P. J. J. Photosensitized Oxidation of Emerging Organic Pollutants by Tetrakis C₆₀
38 Aminofullerene-Derivatized Silica under Visible Light Irradiation. *Environ. Sci. Technol.*
39 **2011**, *45* (24), 10598–10604. <https://doi.org/10.1021/es2029944>.
- 40 (82) Keen, O. S.; Baik, S.; Linden, K. G.; Aga, D. S.; Love, N. G. Enhanced Biodegradation
41 of Carbamazepine after UV/H₂O₂ Advanced Oxidation. *Environ. Sci. Technol.* **2012**, *46*
42 (11), 6222–6227. <https://doi.org/10.1021/es300897u>.
- 43 (83) Brame, J. A.; Hong, S. W.; Lee, J.; Lee, S.-H.; Alvarez, P. J. J. Photocatalytic Pre-
44 Treatment with Food-Grade TiO₂ Increases the Bioavailability and Bioremediation Potential
45 of Weathered Oil from the Deepwater Horizon Oil Spill in the Gulf of Mexico. *Chemosphere*
46 **2013**, *90* (8), 2315–2319. <https://doi.org/10.1016/j.chemosphere.2012.10.009>.
- 47 (84) Saflou, M.; Allahyari, S.; Rahemi, N.; Tasbihi, M. Oil Spill Degradation Using Floating
48 Magnetic Simulated Solar Light-Driven Nano Photocatalysts of Fe₃O₄-ZnO Supported on
49
50
51
52
53
54
55
56
57
58
59
60

- 1
2
3 Lightweight Minerals. *Journal of Environmental Chemical Engineering* **2021**, 9 (4), 105268.
4 <https://doi.org/10.1016/j.jece.2021.105268>.
- 5 (85) Joodi, A.; Allahyari, S.; Rahemi, N.; Hoseini, S.; Tasbihi, M. ZnO–C₃N₄ Solar Light -
6 Driven Nanophotocatalysts on Floating Recycled PET Bottle as Support for Degradation of
7 Oil Spill. *Ceramics International* **2020**, 46 (8), 11328–11339.
8 <https://doi.org/10.1016/j.ceramint.2020.01.162>.
- 9 (86) Hsu, Y.-Y.; Hsiung, T.-L.; Paul Wang, H.; Fukushima, Y.; Wei, Y.-L.; Chang, J.-E.
10 Photocatalytic Degradation of Spill Oils on TiO₂ Nanotube Thin Films. *Marine Pollution*
11 *Bulletin* **2008**, 57 (6), 873–876. <https://doi.org/10.1016/j.marpolbul.2008.03.005>.
- 12 (87) Yang, X.; Yu, J.; Zhang, Y.; Peng, Y.; Li, Z.; Feng, C.; Sun, Z.; Yu, X.; Cheng, J.; Wang,
13 Y. Visible-near-Infrared-Responsive g-C₃N₄H_x+ Reduced Decatungstate with Excellent
14 Performance for Photocatalytic Removal of Petroleum Hydrocarbon. *Journal of Hazardous*
15 *Materials* **2020**, 381, 120994. <https://doi.org/10.1016/j.jhazmat.2019.120994>.
- 16 (88) Qiu, H.; Hu, J.; Zhang, R.; Gong, W.; Yu, Y.; Gao, H. The Photocatalytic Degradation of
17 Diesel by Solar Light-Driven Floating BiOI/EP Composites. *Colloids and Surfaces A:*
18 *Physicochemical and Engineering Aspects* **2019**, 583, 123996.
19 <https://doi.org/10.1016/j.colsurfa.2019.123996>.
- 20 (89) Wang, X.; Wang, J.; Zhang, J.; Louangsouphom, B.; Song, J.; Wang, X.; Zhao, J.
21 Synthesis of Expanded Graphite C/C Composites (EGC) Based Ni-N-TiO₂ Floating
22 Photocatalysts for in Situ Adsorption Synergistic Photocatalytic Degradation of Diesel Oil.
23 *Journal of Photochemistry and Photobiology A: Chemistry* **2017**, 347, 105–115.
24 <https://doi.org/10.1016/j.jphotochem.2017.07.015>.
- 25 (90) Li, Y.; Zhang, Q.; Jiang, J.; Li, L. Long-Acting Photocatalytic Degradation of Crude Oil
26 in Seawater via Combination of TiO₂ and N-Doped TiO₂/Reduced Graphene Oxide.
27 *Environmental Technology* **2021**, 42 (6), 860–870.
28 <https://doi.org/10.1080/09593330.2019.1647291>.
- 29 (91) Hall, G. J.; Fryinger, G. S.; Aeppli, C.; Carmichael, C. A.; Gros, J.; Lemkau, K. L.;
30 Nelson, R. K.; Reddy, C. M. Oxygenated Weathering Products of Deepwater Horizon Oil
31 Come from Surprising Precursors. *Marine Pollution Bulletin* **2013**, 75 (1), 140–149.
32 <https://doi.org/10.1016/j.marpolbul.2013.07.048>.
- 33 (92) Ruddy, B. M.; Huettel, M.; Kostka, J. E.; Lobodin, V. V.; Bythell, B. J.; McKenna, A.
34 M.; Aeppli, C.; Reddy, C. M.; Nelson, R. K.; Marshall, A. G.; Rodgers, R. P. Targeted
35 Petroleomics: Analytical Investigation of Macondo Well Oil Oxidation Products from
36 Pensacola Beach. *Energy Fuels* **2014**, 28 (6), 4043–4050. <https://doi.org/10.1021/ef500427n>.
- 37 (93) Kostka, J. E.; Prakash, O.; Overholt, W. A.; Green, S. J.; Freyer, G.; Canion, A.;
38 Delgardio, J.; Norton, N.; Hazen, T. C.; Huettel, M. Hydrocarbon-Degrading Bacteria and
39 the Bacterial Community Response in Gulf of Mexico Beach Sands Impacted by the
40 Deepwater Horizon Oil Spill. *Appl. Environ. Microbiol.* **2011**, 77 (22), 7962–7974.
41 <https://doi.org/10.1128/AEM.05402-11>.
- 42 (94) Roman-Hubers, A. T.; Aeppli, C.; Dodds, J. N.; Baker, E. S.; McFarlin, K. M.; Letinski,
43 D. J.; Zhao, L.; Mitchell, D. A.; Parkerton, T. F.; Prince, R. C.; Nedwed, T.; Rusyn, I.
44 Temporal Chemical Composition Changes in Water below a Crude Oil Slick Irradiated with
45 Natural Sunlight. *Marine Pollution Bulletin* **2022**, 185, 114360.
46 <https://doi.org/10.1016/j.marpolbul.2022.114360>.
- 47 (95) Lima, B. D.; Martins, L. L.; de Souza, E. S.; Pudenzi, M. A.; da Cruz, G. F. Monitoring
48 Chemical Compositional Changes of Simulated Spilled Brazilian Oils under Tropical
49
50
51
52
53
54
55
56
57
58
59
60

- Climate Conditions by Multiple Analytical Techniques. *Marine Pollution Bulletin* **2021**, *164*, 111985. <https://doi.org/10.1016/j.marpolbul.2021.111985>.
- (96) Chen, H.; Hou, A.; Corilo, Y. E.; Lin, Q.; Lu, J.; Mendelssohn, I. A.; Zhang, R.; Rodgers, R. P.; McKenna, A. M. 4 Years after the *Deepwater Horizon* Spill: Molecular Transformation of Macondo Well Oil in Louisiana Salt Marsh Sediments Revealed by FT-ICR Mass Spectrometry. *Environ. Sci. Technol.* **2016**, *50* (17), 9061–9069. <https://doi.org/10.1021/acs.est.6b01156>.
- (97) Frias, J. P. G. L.; Sobral, P.; Ferreira, A. M. Organic Pollutants in Microplastics from Two Beaches of the Portuguese Coast. *Marine Pollution Bulletin* **2010**, *60* (11), 1988–1992. <https://doi.org/10.1016/j.marpolbul.2010.07.030>.
- (98) *Unique Molecular Features of Water-Soluble Photo-Oxidation Products among Refined Fuels, Crude Oil, and Herded Burnt Residue under High Latitude Conditions | ACS ES&T Water*. <https://pubs.acs.org/doi/abs/10.1021/acsestwater.1c00494> (accessed 2023-09-05).
- (99) Tarr, M. A.; Zito, P.; Overton, E. B.; Olson, G. M.; Adhikari, P. L.; Reddy, C. M. Weathering of Oil Spilled in the Marine Environment. *Oceanography* **2016**, *29* (3), 126–135.
- (100) Ward, C. P.; Sharpless, C. M.; Valentine, D. L.; French-McCay, D. P.; Aeppli, C.; White, H. K.; Rodgers, R. P.; Gosselin, K. M.; Nelson, R. K.; Reddy, C. M. Partial Photochemical Oxidation Was a Dominant Fate of Deepwater Horizon Surface Oil. *Environ. Sci. Technol.* **2018**, *9*.
- (101) Rontani, J.-F.; Rabourdin, A.; Aubert, C. Electron Ionization Mass Spectral Fragmentation of Some Isoprenoid Glycidic Ethers. *Rapid Communications in Mass Spectrometry* **2001**, *15* (22), 2091–2095. <https://doi.org/10.1002/rcm.484>.
- (102) Alonso, M. C.; Barceló, D. Tracing Polar Benzene- and Naphthalenesulfonates in Untreated Industrial Effluents and Water Treatment Works by Ion-Pair Chromatography-Fluorescence and Electrospray-Mass Spectrometry. *Analytica Chimica Acta* **1999**, *400* (1), 211–231. [https://doi.org/10.1016/S0003-2670\(99\)00705-9](https://doi.org/10.1016/S0003-2670(99)00705-9).
- (103) Cawley, K. M.; Hakala, J. A.; Chin, Y.-P. Evaluating the Triplet State Photoreactivity of Dissolved Organic Matter Isolated by Chromatography and Ultrafiltration Using an Alkylphenol Probe Molecule. *Limnology and Oceanography: Methods* **2009**, *7* (6), 391–398. <https://doi.org/10.4319/lom.2009.7.391>.
- (104) Zepp, R. G.; Schlotzhauer, P. F.; Sink, R. Merritt. Photosensitized Transformations Involving Electronic Energy Transfer in Natural Waters: Role of Humic Substances. *Environ. Sci. Technol.* **1985**, *19* (1), 74–81. <https://doi.org/10.1021/es00131a008>.
- (105) Kim, D.; Ha, S. Y.; An, J. G.; Cha, S.; Yim, U. H.; Kim, S. Estimating Degree of Degradation of Spilled Oils Based on Relative Abundance of Aromatic Compounds Observed by Paper Spray Ionization Mass Spectrometry. *Journal of Hazardous Materials* **2018**, *359*, 421–428. <https://doi.org/10.1016/j.jhazmat.2018.07.060>.
- (106) Islam, A.; Cho, Y.; Yim, U. H.; Shim, W. J.; Kim, Y. H.; Kim, S. The Comparison of Naturally Weathered Oil and Artificially Photo-Degraded Oil at the Molecular Level by a Combination of SARA Fractionation and FT-ICR MS. *Journal of Hazardous Materials* **2013**, *263*, 404–411. <https://doi.org/10.1016/j.jhazmat.2013.09.030>.
- (107) Bobinger, S.; Andersson, J. T. Photooxidation Products of Polycyclic Aromatic Compounds Containing Sulfur. *Environ. Sci. Technol.* **2009**, *43* (21), 8119–8125. <https://doi.org/10.1021/es901859s>.
- (108) Neuman, J. A.; Aikin, K. C.; Atlas, E. L.; Blake, D. R.; Holloway, J. S.; Meinardi, S.; Nowak, J. B.; Parrish, D. D.; Peischl, J.; Perring, A. E.; Pollack, I. B.; Roberts, J. M.;

- Ryerson, T. B.; Trainer, M. Ozone and Alkyl Nitrate Formation from the Deepwater Horizon Oil Spill Atmospheric Emissions. *Journal of Geophysical Research: Atmospheres* **2012**, *117* (D9). <https://doi.org/10.1029/2011JD017150>.
- (109) Schmidl, C.; Marr, I. L.; Caseiro, A.; Kotianová, P.; Berner, A.; Bauer, H.; Kasper-Giebl, A.; Puxbaum, H. Chemical Characterisation of Fine Particle Emissions from Wood Stove Combustion of Common Woods Growing in Mid-European Alpine Regions. *Atmospheric Environment* **2008**, *42* (1), 126–141. <https://doi.org/10.1016/j.atmosenv.2007.09.028>.
- (110) Parvez, S.; Venkataraman, C.; Mukherji, S. A Review on Advantages of Implementing Luminescence Inhibition Test (*Vibrio Fischeri*) for Acute Toxicity Prediction of Chemicals. *Environment International* **2006**, *32* (2), 265–268. <https://doi.org/10.1016/j.envint.2005.08.022>.
- (111) Zito, P.; Podgorski, D. C.; Johnson, J.; Chen, H.; Rodgers, R. P.; Guillemette, F.; Kellerman, A. M.; Spencer, R. G. M.; Tarr, M. A. Molecular-Level Composition and Acute Toxicity of Photosolubilized Petrogenic Carbon. *Environ. Sci. Technol.* **2019**, *53* (14), 8235–8243. <https://doi.org/10.1021/acs.est.9b01894>.
- (112) Kim, D.; Jung, J.-H.; Ha, S. Y.; An, J. G.; Shankar, R.; Kwon, J.-H.; Yim, U. H.; Kim, S. H. Molecular Level Determination of Water Accommodated Fraction with Embryonic Developmental Toxicity Generated by Photooxidation of Spilled Oil. *Chemosphere* **2019**, *237*, 124346. <https://doi.org/10.1016/j.chemosphere.2019.124346>.
- (113) Harriman, B. H.; Zito, P.; Podgorski, D. C.; Tarr, M. A.; Suflita, J. M. Impact of Photooxidation and Biodegradation on the Fate of Oil Spilled During the Deepwater Horizon Incident: Advanced Stages of Weathering. *Environ. Sci. Technol.* **2017**, *10*.
- (114) Prince, R. C.; Garrett, R. M.; Bare, R. E.; Grossman, M. J.; Townsend, T.; Suflita, J. M.; Lee, K.; Owens, E. H.; Sergy, G. A.; Braddock, J. F.; Lindstrom, J. E.; Lessard, R. R. The Roles of Photooxidation and Biodegradation in Long-Term Weathering of Crude and Heavy Fuel Oils. *Spill Science & Technology Bulletin* **2003**, *8* (2), 145–156. [https://doi.org/10.1016/S1353-2561\(03\)00017-3](https://doi.org/10.1016/S1353-2561(03)00017-3).
- (115) Bacosa, H. P.; Liu, Z.; Erdner, D. L. Natural Sunlight Shapes Crude Oil-Degrading Bacterial Communities in Northern Gulf of Mexico Surface Waters. *Frontiers in Microbiology* **2015**, *6*.
- (116) Fenn, J. B.; Mann, M.; Meng, C. K.; Wong, S. F.; Whitehouse, C. M. Electrospray Ionization for Mass Spectrometry of Large Biomolecules. *Science* **1989**, *246* (4926), 64–71.
- (117) Stanford, L. A.; Kim, S.; Klein, G. C.; Smith, D. F.; Rodgers, R. P.; Marshall, A. G. Identification of Water-Soluble Heavy Crude Oil Organic-Acids, Bases, and Neutrals by Electrospray Ionization and Field Desorption Ionization Fourier Transform Ion Cyclotron Resonance Mass Spectrometry. *Environ. Sci. Technol.* **2007**, *41* (8), 2696–2702. <https://doi.org/10.1021/es0624063>.
- (118) Smith, D. F.; Podgorski, D. C.; Rodgers, R. P.; Blakney, G. T.; Hendrickson, C. L. 21 Tesla FT-ICR Mass Spectrometer for Ultrahigh-Resolution Analysis of Complex Organic Mixtures. *Anal. Chem.* **2018**, *90* (3), 2041–2047. <https://doi.org/10.1021/acs.analchem.7b04159>.
- (119) McKenna, A. M.; Blakney, G. T.; Xian, F.; Glaser, P. B.; Rodgers, R. P.; Marshall, A. G. Heavy Petroleum Composition. 2. Progression of the Boduszynski Model to the Limit of Distillation by Ultrahigh-Resolution FT-ICR Mass Spectrometry. *Energy Fuels* **2010**, *24* (5), 2939–2946. <https://doi.org/10.1021/ef1001502>.

- 1
2
3 (120) Rodgers, R. P.; McKenna, A. M. Petroleum Analysis. *Anal. Chem.* **2011**, 83 (12), 4665–
4 4687. <https://doi.org/10.1021/ac201080e>.
- 5 (121) McKenna, A. M.; Nelson, R. K.; Reddy, C. M.; Savory, J. J.; Kaiser, N. K.; Fitzsimmons,
6 J. E.; Marshall, A. G.; Rodgers, R. P. Expansion of the Analytical Window for Oil Spill
7 Characterization by Ultrahigh Resolution Mass Spectrometry: Beyond Gas Chromatography.
8 *Environ. Sci. Technol.* **2013**, 47 (13), 7530–7539. <https://doi.org/10.1021/es305284t>.
- 9 (122) Boduszynski, M. M. Composition of Heavy Petroleum. 2. Molecular Characterization.
10 *Energy Fuels* **1988**, 2 (5), 597–613. <https://doi.org/10.1021/ef00011a001>.
- 11 (123) Altgelt, K. H. *Composition and Analysis of Heavy Petroleum Fractions*; CRC Press,
12 1993.
- 13 (124) Podgorski, D. C.; Corilo, Y. E.; Nyadong, L.; Lobodin, V. V.; Bythell, B. J.; Robbins, W.
14 K.; McKenna, A. M.; Marshall, A. G.; Rodgers, R. P. Heavy Petroleum Composition. 5.
15 Compositional and Structural Continuum of Petroleum Revealed. *Energy Fuels* **2013**, 27 (3),
16 1268–1276. <https://doi.org/10.1021/ef301737f>.
- 17 (125) Corilo, Y. E.; Podgorski, D. C.; McKenna, A. M.; Lemkau, K. L.; Reddy, C. M.;
18 Marshall, A. G.; Rodgers, R. P. Oil Spill Source Identification by Principal Component
19 Analysis of Electrospray Ionization Fourier Transform Ion Cyclotron Resonance Mass
20 Spectra. *Anal. Chem.* **2013**, 85 (19), 9064–9069. <https://doi.org/10.1021/ac401604u>.
- 21 (126) P. Barrow, M.; I. Burkitt, W.; J. Derrick, P. Principles of Fourier Transform Ion
22 Cyclotron Resonance Mass Spectrometry and Its Application in Structural Biology. *Analyst*
23 **2005**, 130 (1), 18–28. <https://doi.org/10.1039/B403880K>.
- 24 (127) *Fourier transform ion cyclotron resonance mass spectrometry: A primer - Marshall -*
25 *1998 - Mass Spectrometry Reviews - Wiley Online Library.*
26 [https://onlinelibrary.wiley.com/doi/abs/10.1002/\(SICI\)1098-2787\(1998\)17:1%3C1::AID-](https://onlinelibrary.wiley.com/doi/abs/10.1002/(SICI)1098-2787(1998)17:1%3C1::AID-)
27 [MAS1%3E3.0.CO;2-K](https://onlinelibrary.wiley.com/doi/abs/10.1002/(SICI)1098-2787(1998)17:1%3C1::AID-) (accessed 2020-08-12).
- 28 (128) Robb, D. B.; Blades, M. W. Atmospheric Pressure Photoionization for Ionization of Both
29 Polar and Nonpolar Compounds in Reversed-Phase LC/MS. *Anal. Chem.* **2006**, 78 (23),
30 8162–8164. <https://doi.org/10.1021/ac061276d>.
- 31 (129) Raffaelli, A.; Saba, A. Atmospheric Pressure Photoionization Mass Spectrometry. *Mass*
32 *Spectrometry Reviews* **2003**, 22 (5), 318–331. <https://doi.org/10.1002/mas.10060>.
- 33 (130) Vaughan, P. P.; Wilson, T.; Kamerman, R.; Hagy, M. E.; McKenna, A.; Chen, H.;
34 Jeffrey, W. H. Photochemical Changes in Water Accommodated Fractions of MC252 and
35 Surrogate Oil Created during Solar Exposure as Determined by FT-ICR MS. *Marine*
36 *Pollution Bulletin* **2016**, 104 (1–2), 262–268.
37 <https://doi.org/10.1016/j.marpolbul.2016.01.012>.
- 38 (131) Klein, G. C.; Angström, A.; Rodgers, R. P.; Marshall, A. G. Use of
39 Saturates/Aromatics/Resins/Asphaltenes (SARA) Fractionation To Determine Matrix Effects
40 in Crude Oil Analysis by Electrospray Ionization Fourier Transform Ion Cyclotron
41 Resonance Mass Spectrometry. *Energy Fuels* **2006**, 20 (2), 668–672.
42 <https://doi.org/10.1021/ef050353p>.
- 43 (132) *Handbook of Petroleum Analysis*. Wiley Analytical Science.
44 <https://analyticalscience.wiley.com/do/10.1002/sepspec.9780471361671> (accessed 2022-07-
45 06).
- 46 (133) Ventura, G. T.; Raghuraman, B.; Nelson, R. K.; Mullins, O. C.; Reddy, C. M. Compound
47 Class Oil Fingerprinting Techniques Using Comprehensive Two-Dimensional Gas
48
49
50
51
52
53
54
55
56
57
58
59
60

- Chromatography (GC×GC). *Organic Geochemistry* **2010**, *41* (9), 1026–1035.
<https://doi.org/10.1016/j.orggeochem.2010.02.014>.
- (134) Lemkau, K. L.; Peacock, E. E.; Nelson, R. K.; Ventura, G. T.; Kovacs, J. L.; Reddy, C. M. The M/V Cosco Busan Spill: Source Identification and Short-Term Fate. *Marine Pollution Bulletin* **2010**, *60* (11), 2123–2129.
<https://doi.org/10.1016/j.marpolbul.2010.09.001>.
- (135) Wang, H.; Manicke, N. E.; Yang, Q.; Zheng, L.; Shi, R.; Cooks, R. G.; Ouyang, Z. Direct Analysis of Biological Tissue by Paper Spray Mass Spectrometry. *Anal. Chem.* **2011**, *83* (4), 1197–1201. <https://doi.org/10.1021/ac103150a>.
- (136) *Paper Spray Chemical Ionization: Highly Sensitive Ambient Ionization Method for Low- and Nonpolar Aromatic Compounds | Analytical Chemistry*.
https://pubs.acs.org/doi/abs/10.1021/acs.analchem.7b01733?casa_token=zdXEb5FUHUAAA:AAA:Hf8Ks7P3aiXFBodnkMBVG8xd05NISm_FNsFNG4ZnXtZr6YVGLinxDmAVNUNz25dzqlWz1TtraA7Q6ze2 (accessed 2020-08-13).
- (137) Lobodin, V. V.; Maksimova, E. V.; Rodgers, R. P. Gas Chromatography/Atmospheric Pressure Chemical Ionization Tandem Mass Spectrometry for Fingerprinting the Macondo Oil Spill. *Anal. Chem.* **2016**, *88* (13), 6914–6922.
<https://doi.org/10.1021/acs.analchem.6b01652>.
- (138) Técnica, O.; Accidentales, V. M. Oil Spill Environmental Forensics: Fingerprinting and Source Identification.....26.
- (139) Aeppli, C.; Nelson, R. K.; Radović, J. R.; Carmichael, C. A.; Valentine, D. L.; Reddy, C. M. Recalcitrance and Degradation of Petroleum Biomarkers upon Abiotic and Biotic Natural Weathering of Deepwater Horizon Oil. *Environ. Sci. Technol.* **2014**, *48* (12), 6726–6734.
<https://doi.org/10.1021/es500825q>.
- (140) Arey, J. S.; Nelson, R. K.; Reddy, C. M. Disentangling Oil Weathering Using GC×GC. 1. Chromatogram Analysis. *Environ. Sci. Technol.* **2007**, *41* (16), 5738–5746.
<https://doi.org/10.1021/es070005x>.
- (141) Lemkau, K. L.; McKenna, A. M.; Podgorski, D. C.; Rodgers, R. P.; Reddy, C. M. Molecular Evidence of Heavy-Oil Weathering Following the M/V *Cosco Busan* Spill: Insights from Fourier Transform Ion Cyclotron Resonance Mass Spectrometry. *Environ. Sci. Technol.* **2014**, *48* (7), 3760–3767. <https://doi.org/10.1021/es403787u>.
- (142) Hughey, C. A.; Minardi, C. S.; Galasso-Roth, S. A.; Paspalof, G. B.; Mapolelo, M. M.; Rodgers, R. P.; Marshall, A. G.; Ruderman, D. L. Naphthenic Acids as Indicators of Crude Oil Biodegradation in Soil, Based on Semi-Quantitative Electrospray Ionization Fourier Transform Ion Cyclotron Resonance Mass Spectrometry. *Rapid Communications in Mass Spectrometry* **2008**, *22* (23), 3968–3976. <https://doi.org/10.1002/rcm.3813>.
- (143) Arekhi, M.; Terry, L. G.; John, G. F.; Clement, T. P. Environmental Fate of Petroleum Biomarkers in Deepwater Horizon Oil Spill Residues over the Past 10 Years. *Science of The Total Environment* **2021**, *791*, 148056. <https://doi.org/10.1016/j.scitotenv.2021.148056>.